Ultrasound of the Liver
Malignant Liver Lesions

Dirk-André Clevert
Interdisciplinary Ultrasound Center at the Munich University Hospital – Grosshadern (Germany)

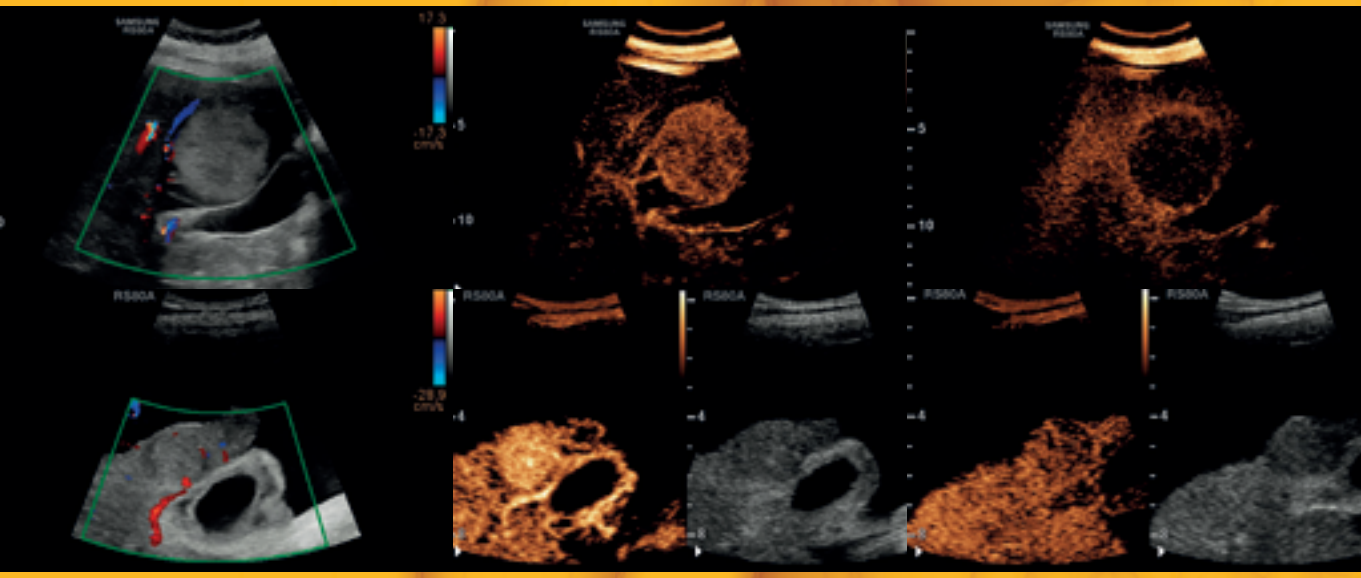

The information contained in this brochure is intended exclusively for physicians and pharmacists. The contents reflect current developments in medical science. For information on indications and dosage schemes of the drugs please refer to the current SPCs (summary of product characteristics). Product presentations, compositions, indications and safety information as referenced herein may differ from those in your country. For further information, please contact Dr. Falk Pharma GmbH, Freiburg (Germany) or your local Falk partner.

Publisher

FALK FOUNDATION e.V.

Leinenweberstr. 5
79108 Freiburg
Germany

www.falkfoundation.org

Image credits

Cover: Magic mine/Shutterstock
All figures: Dirk-André Clevert

1st edition 2020

Ultrasound of the Liver

Malignant Liver Lesions

Dirk-André Clevert
Interdisciplinary Ultrasound Center at the Munich University Hospital – Grosshadern (Germany)

Address of the author

Prof. Dr. Dr. h. c. (TSM-Univ.) Dirk-André Clevert
Interdisciplinary Ultrasound Center
Department of Clinical Radiology
Munich University Hospital – Grosshadern
Marchioninistr. 15
81377 Munich
Germany
dirk.clevert@med.uni-muenchen.de

Contents

Foreword

This booklet is intended both for physicians who use contrast-enhanced ultrasound (CEUS) in their daily clinical practice and for those who would like to learn this new technique. Using real-life examples, the booklet will illustrate the enhancement properties of numerous types of malignant liver tumors, first using B-mode, color Doppler, or power Doppler imaging and then using CEUS. The CEUS images of these malignant liver lesions will then be discussed in depth, specifically the pattern of the contrast medium in each type of lesion during the arterial, portal venous, and late phases. The objective of this booklet is to provide the reader a brief introduction to this topic together with a comprehensive collection of images of these varied hepatic pathologies.

1 Introduction

Ultrasound is typically the first imaging modality used to diagnose liver lesions, and is performed using multifrequency ultrasound transducers with a range of 1–9 MHz. Many ultrasound devices currently optimize B-mode imaging by providing standard features such as tissue harmonic imaging (THI) in harmonic frequency ranges and speckle reduction imaging (SRI), which optimizes the delineation of tissue contours by reducing speckle. Modern devices can further adjust B-mode images to various brightness conditions, and many also provide colorization. These technical developments may help characterize lipodystrophies, pathologies of the intrahepatic bile ducts, diffuse nodular lesions, and even early and advanced parenchymal abnormalities [Clevert et al. 2011, 2013; Jung et al. 2012; Yen et al. 2008].

2 Contrast-enhanced ultrasound (CEUS)

Contrast-enhanced ultrasound (CEUS) is performed by injecting patients with small quantities (1.0–2.4 ml) of a special ultrasound contrast agent as an intravenous bolus, followed immediately by intravenous injection of about 10 ml of 0.9% saline solution [Clevert et al. 2009]. This contrast agent consists of microbubbles 1–10 µm in size containing the inert gas sulfur hexafluoride and stabilized by a phospholipid shell. Unlike the conventional contrast agents used for computed tomography (CT) and magnetic resonance imaging (MRI), CEUS contrast agents do not extravasate into interstitial spaces but rather remain within the vascular system, allowing organ perfusion to be visualized [Claudon et al. 2013; Greis 2009; Lindner et al. 2002]. The acoustic impedance of the gas in the microbubbles differs greatly from that of blood, triggering backscatter of the incoming ultrasound waves at the surface of the microbubbles. Furthermore, due to their specific properties the microbubbles also oscillate, which generates a non-linear contrast-specific signal [Greis 2009].

Ultrasound scanners with contrast-specific software can discriminate between the linear signal reflected by tissue and the non-linear responses from microbubbles, allowing them to generate images with pixel intensities that correspond to the local concentration of the ultrasound contrast agent [Claudon et al. 2013].

Continuous recording is essential during the arterial phase, after which it is recommended that images only be recorded intermittently every 30 seconds until the late phase in order to minimize microbubble destruction by the ultrasound waves. The phospholipid component of the microbubbles (the stabilizing shell) is metabolized by the liver while the gas is exhaled by the lungs. There is no risk of nephrotoxicity [Piscaglia et al. 2006].

The main advantage of CEUS is the fact that the injected contrast agent allows microvascular blood flows with a diameter of approximately 10 µm to be visualized [Claudon et al. 2002]. The liver receives a dual blood supply from the hepatic artery and the portal vein. The portal vein transports venous blood from the gastrointestinal tract and the spleen and is responsible for 70–75% of the blood supply to the liver, while the remaining 25–30% is provided by the hepatic artery.

This dual blood supply of liver parenchyma allows the vascularization of the liver to be visualized across **three distinct contrast phases** when microbubbles are used [Claudon et al. 2013, Nicolau et al. 2006]:

I. **Arterial phase:** The arterial phase starts within 10–20 seconds after injection and lasts 35–40 seconds.

II. **Portal venous phase:** The portal venous phase is characterized by the inflow of contrast agent through the portal vein and commences 30–45 seconds after injection.

III. **Late phase:** The late phase starts about 120 seconds after the injection of contrast agent. During this phase, the overall echogenicity of the liver becomes more intense. Since the microbubbles do not extravasate from blood vessels, there is no interstitial phase (as with CT or MRI), and enhancement continuously decreases over the remaining observation period (late phase) [Claudon et al. 2013].

It is recommended that video recordings of the entire liver be captured during all three contrast phases as it is not possible to examine multiple lesions simultaneously during the arterial or portal venous phases [Nicolau et al. 2006].

The late phase of CEUS is especially useful for detecting metastases, and it also enables ultrasound-based staging of liver tumors in oncology patients. Nonetheless, very small, simple cysts may also potentially be misinterpreted as suspected metastases during the late phase since both types of lesions take up less contrast than the surrounding parenchyma during this phase. This phenomenon clearly shows why comprehensive B-mode and color Doppler examinations are indispensable prior to performing CEUS [Jung & Clevert 2018; Müller-Peltzer et al. 2017, 2018; Negrão de Figueiredo et al. 2018].

Similar to contrast-enhanced CT and MRI, CEUS can also be used to detect and characterize liver lesions. It allows the vascularization of focal liver lesions to be evaluated in real-time with a high degree of spatial resolution [Nicolau et al. 2006]. Ultrasound contrast agents do not exhibit any cardio-, hepato-, or nephrotoxic effects, and administration of these agents has no effects on thyroid function. Accordingly, the incidence of anaphylactic reactions is reported to be 1/10,000, which is lower than that of CT contrast agents [Claudon et al. 2013; Piscaglia et al. 2006].

Despite these major benefits, the use of CEUS in the liver is also associated with some limitations. Due to the limited resolution of the technique, very small lesions below the detection limit of 3–5 mm may be overlooked. Furthermore, it may not be possible to visualize lesions in localizations of the liver that are difficult to image using ultrasound, such as in the subdiaphragmatic regions of segment VIII. CEUS also has a limited penetration depth, making it difficult to detect deep-seated lesions or lesions in patients with steatosis [Claudon et al. 2013]. As with native B-mode ultrasound, the informative power of the method may be greatly reduced in patients with obesity or abdominal distension. In addition to such patient-specific variables, the diagnostic reliability of CEUS also depends on the expertise of the examiner [Chiorean et al. 2016; Müller-Peltzer et al. 2017].

3 Malignant liver lesions

3.1 Liver metastases

Focal liver lesions are very common, with a prevalence of approximately 5% in the general population [Strobel 2006]. In 25–50% of all cancer patients, the primary tumor has already metastasized to the liver by the time of diagnosis [Oldenburg et al. 2005]. The appearance of metastases in ultrasound may vary greatly and is primarily determined by their echogenicity relative to the surrounding parenchyma (Table 1). It is typically possible to detect focal metastases with a diameter of 5–10 mm or larger. CT may be a superior modality for detecting metastases with unfavorable localizations (subphrenic space, left upper lobe, lateral far right). The size, number, and location of liver metastases are the key criteria used when selecting a treatment strategy (surgical resection vs. liver-directed therapy) [Harvey et al. 2001]. A reliable method to detect and characterize focal liver lesions is indispensable for determining both a patient's prognosis and treatment [Regge et al. 2006] (Table 2).

Liver metastases represent the vast majority of the masses detected in the liver of cancer patients. These patients typically have multiple liver metastases (> 90%) rather than only a single metastasis (< 10%) [Weskott 2010].

In the vast majority of cases, metastases are found in both lobes (77%) instead of only in the right lobe (20%) or left lobe (3%) of the liver. Thirty percent of metastatic lesions in the liver are smaller than 10 mm. Even in patients with malignant cancer, 80% of all lesions smaller than 15 mm have been shown to be benign [Jones et al. 1992].

The introduction of contrast-enhanced ultrasound (CEUS) in 2001 revolutionized the diagnostic reliability of ultrasound.

This method uses contrast enhancement to characterize changes in the appearance of focal liver lesions relative to their surrounding tissue over time. The criteria set out by the European Federation of Societies for Ultrasound in Medicine and Biology (EFSUMB) define three phases of contrast enhancement. The arterial phase starts 10–20 seconds after the intravenous injection of contrast agent and reveals the extent and pattern of arterial blood flow. The portal venous phase then commences after 30–45 seconds and transitions to the late phase after about 120 seconds [Claudon et al. 2013; Müller-Peltzer et al. 2017] (Tables 3–5).

Benign, solid, focal liver lesions exhibit sustained enhancement during the portal venous and late phases, and can be further characterized by their enhancement patterns during the arterial phase.

A meta-analysis by Kinkel et al. reported that B-mode ultrasound has a detection rate of only 55% for liver metastasis originating from gastrointestinal tumors, compared with detection rates of 72% for contrast-enhanced CT, 76% for contrast-enhanced MRI, and 90% for positron emission tomography (PET) [Kinkel et al. 2002; Weskott 2011].

However, CEUS and the CHI (contrast harmonic imaging) technique allow > 95% of liver lesions to be detected and > 90% to be characterized, thus achieving a level of diagnostic reliability on par with that of contrast-enhanced CT [Clevert et al. 2009; Dörffel & Wermke 2008; Ladam-Marcus et al. 2009; Müller-Peltzer et al. 2017; Nicolau et al. 2006].

A multicenter study at 24 hospitals in Germany demonstrated that CEUS is a very reliable imaging modality for characterizing focal liver lesions, achieving a diagnostic accuracy of 90.3%. Using CEUS, malignant lesions could be detected with a sensitivity of 95.8% and benign lesions could be detected with a specificity of 83.1%. The positive predictive value for the diagnosis of a malignant tumor was 95.4% in this study, while the negative predictive value was 95.7% [Strobel et al. 2008] (Table 6).

A subgroup analysis of this German multicenter study revealed that CEUS has a diagnostic accuracy of 83.8% for histologically-confirmed liver lesions ≤ 20 mm (n = 241). The sensitivity for malignant lesions was 93.5% and the specificity for benign lesions was 66.7%. The positive predictive value of CEUS for malignant liver lesions was 92.3%, while the negative predictive value was 95.1% [Strobel et al. 2011].

Due to their arterial blood supply and the absence of portal blood supply, liver metastases exhibit a typical pattern of contrast accumulation. Following administration of the contrast agent, metastases initially appear as hypervascular or hypovascular lesions depending on the form of primary tumor, after which the contrast agent begins to accumulate much more gradually in the surrounding liver parenchyma. In addition to contrast enhancement by the tumor tissue itself, the arteries supplying the tumor and the intralesional blood vessels may also become visible. Contrast

enhancement of tumors decreases during the portal venous phase, and during the late phase the vast majority of liver metastases appear hypoechoic or anechoic relative to the surrounding healthy parenchyma [Weskott 2010] (Figs. 1–45).

Nodular micrometastases	Not visible by ultrasound
Diffuse infiltration	Not visible by ultrasound
Diffuse infiltration with liver enlargement	
Nodular metastases with equivalent echogenicity as liver tissue:	
Visible	– As a protrusion on the surface of the liver
	– By displacement or compression of blood vessels
	– By changes in echogenicity over time
Road map-like infiltration	
Appearance of foci:	
– Anechoic with posterior acoustic enhancement	
– Hypoechoic with or without rim	
– Echogenic with or without rim	
– Hyperechoic with anechoic or echogenic internal space (spontaneously or secondary to treatment)	
– Regressive pathologies (scarring, calcification, necrosis)	

Table 1: Appearance of liver metastases using conventional B-mode ultrasound.

If suspected metastatic lesions are detected:
– Reliability of diagnosis
– Feasibility of biopsy
– Number, localization (which segment), and size in the context of resection
– Spread to lymph nodes or infiltration into adjacent organs
– Number, localization, size, and sonographic appearance in the context of follow-up during treatment (reference lesions)
– Are other examinations required (in case of limited ultrasound quality or small lesions)

Table 2: Criteria for determining metastasis using ultrasound [Ochs 2014].

Hypervascular liver lesions
– Neuroendocrine tumors
– Carcinoid tumors
– Thyroid cancer
– Renal cell carcinoma
– Breast cancer
– Melanoma
– Urothelial carcinoma
– Sarcoma
– Lymphoma

Table 3: The most common forms of hypervascularity among liver metastases. Breast tumors, lymphoma, and melanoma may be either hypervascular or hypovascular (modified from [Prokop et al. 2003]).

Hypovascular liver lesions
– Adenocarcinoma (gastrointestinal tract, lungs)
– Breast cancer
– Squamous cell carcinoma
– Lymphoma

Table 4: The most common forms of hypovascularity among liver metastases (modified from [Prokop et al. 2003]).

Lesion	Arterial phase	Portal venous phase	Late phase
Typical signs	Rim enhancement	Hypo-enhancement	Hypo-enhancement to non-enhancement
Other findings	Complete enhancement, hyper-enhancement, regions without enhancement	Regions without enhancement	Regions without enhancement

Table 5: Enhancement patterns of liver metastases [Claudon et al. 2013].

Diagnostic accuracy	90.3%
Sensitivity	95.8%
Specificity	83.1%
Positive predictive value for malignancy	95.4%
Negative predictive value for malignancy	95.7%

Table 6: The DEGUM multicenter study enrolled 1,349 patients with 573 benign and 744 malignant focal liver lesions. The diagnoses were confirmed by biopsy in 75% of cases and by other imaging modalities such as CT or MRI in 25% of cases [Strobel et al. 2008].

3.1.1 Case reviews – Liver metastases

Case review 1

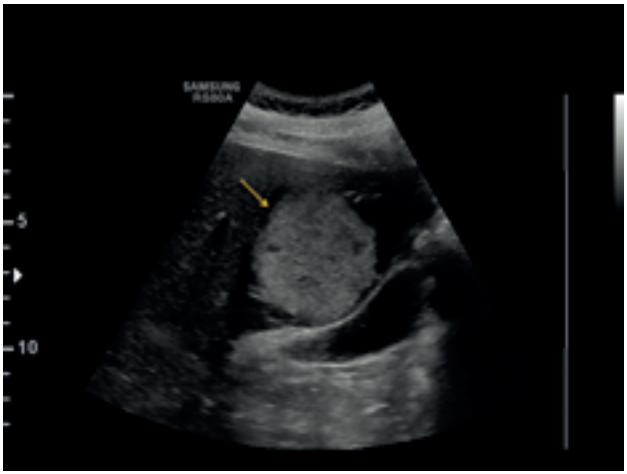

Figure 1: 36-year-old male patient with large, hyperechoic lesion (yellow arrow) in a non-cirrhotic liver.

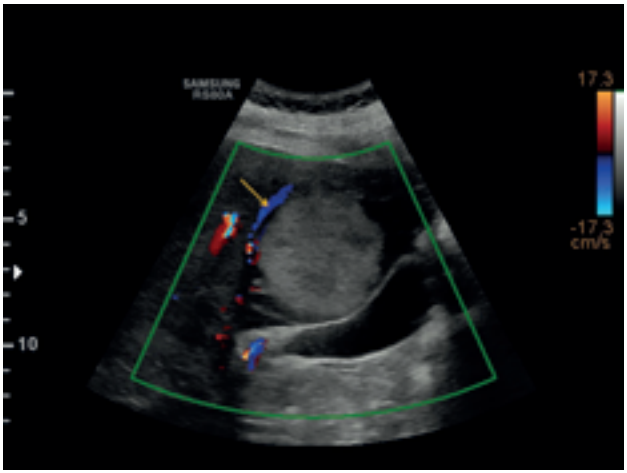

Figure 2: The hyperechoic lesion (yellow arrow) does not display any increase in vascularization in color duplex sonography.

Figure 3: Contrast-enhanced ultrasound. In the **arterial phase**, the lesion is delineated by intense enhancement (yellow arrow).

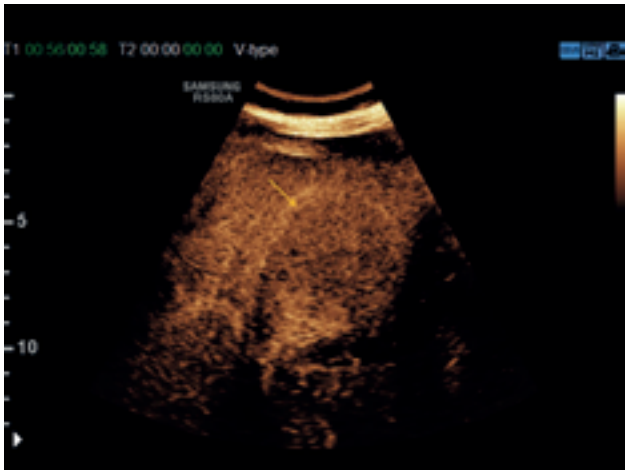

Figure 4: In the **portal venous phase** after approx. 56 seconds, incipient wash-out of the lesion (yellow arrow) allows it to be distinguished from the surrounding liver tissue.

Figure 5: In the **late phase** after over 2 minutes, the lesion (yellow arrow) stands out from the surrounding liver tissue following intense wash-out. The lesion was confirmed by histology as a metastasis originating from a neuroendocrine tumor of the pancreas.

Case review 2

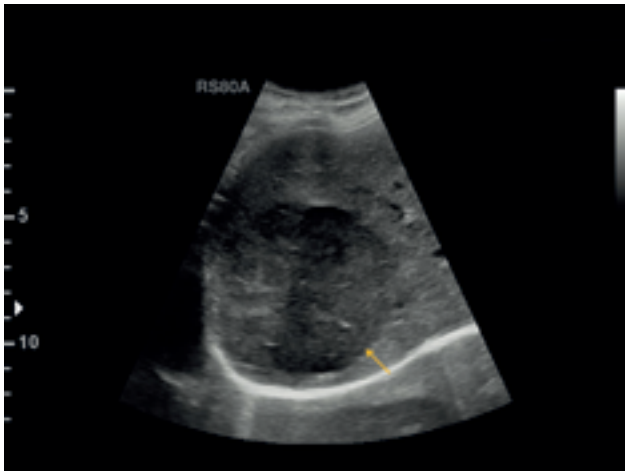

Figure 6: 38-year-old female patient with a large, hypoechoic lesion (yellow arrow) in the right lobe of the liver. A CT performed at another facility led to a diagnosis of suspected hemangioma.

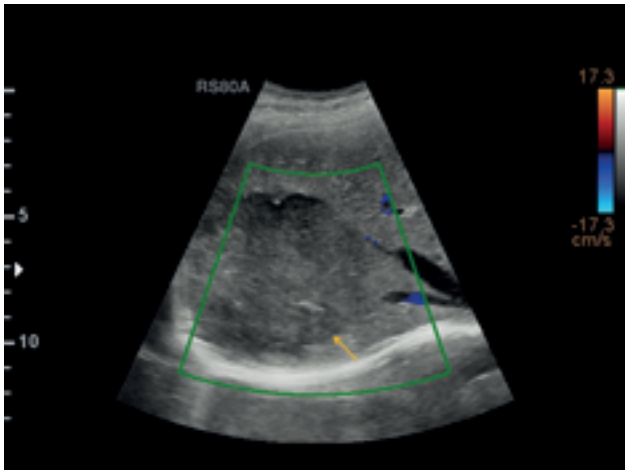

Figure 7: The hypoechoic lesion (yellow arrow) does not display any increase in vascularization in color duplex sonography.

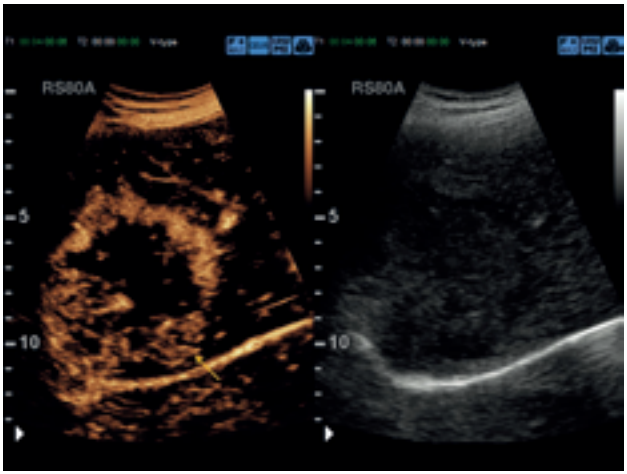

Figure 8: Contrast-enhanced ultrasound. In the **arterial phase**, the lesion is delineated by intense marginal enhancement (yellow arrow).

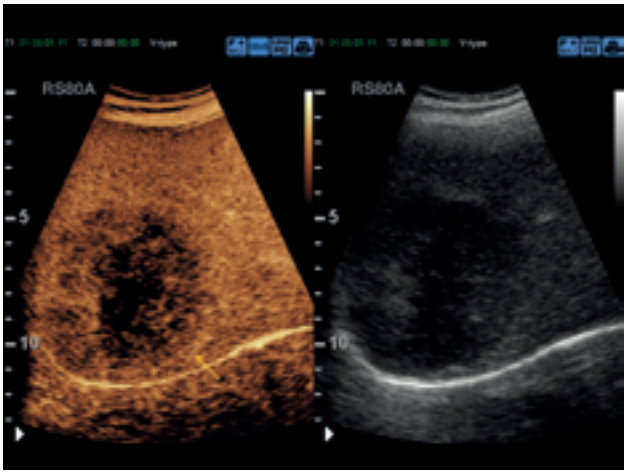

Figure 9: In the **portal venous phase** after approx. 1 minute, incipient wash-out of the margins of the lesion (yellow arrow) allows it to be distinguished from the surrounding liver tissue. The central regions of the lesion display no uptake of contrast agent.

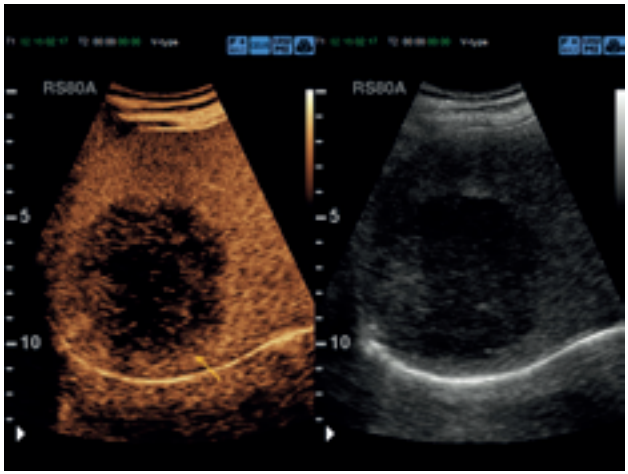

Figure 10: In the **late phase** after over 2 minutes, the lesion (yellow arrow) stands out from the surrounding liver tissue following intense wash-out. The lesion was confirmed by histology as a metastasis originating from breast cancer.

Case review 3

Figure 11: 65-year-old male patient with a small, hypoechoic lesion (yellow arrow) in the right lobe of the liver. A CT performed at another facility led to a diagnosis of a suspected complex cyst, and contrast-enhanced ultrasound was recommended.

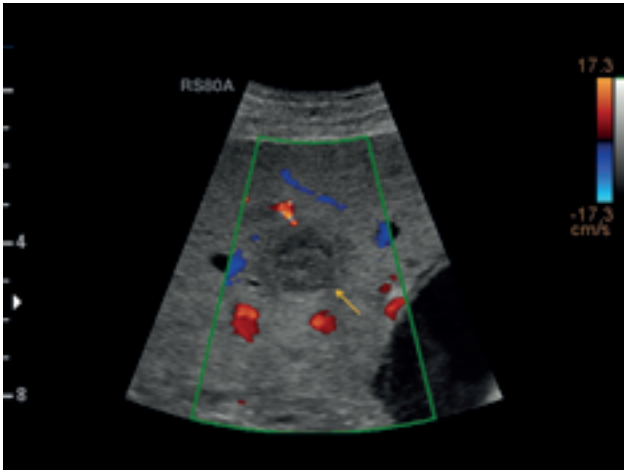

Figure 12: The hypoechoic lesion (yellow arrow) does not display any increase in vascularization in color duplex sonography.

Figure 13: Contrast-enhanced ultrasound. In the **arterial phase**, the lesion is delineated by intense marginal enhancement (yellow arrow).

Figure 14: In the **portal venous phase**, incipient wash-out of the margins of the lesion (yellow arrow) allows it to be distinguished from the surrounding liver tissue. The central regions of the lesion display no uptake of contrast agent.

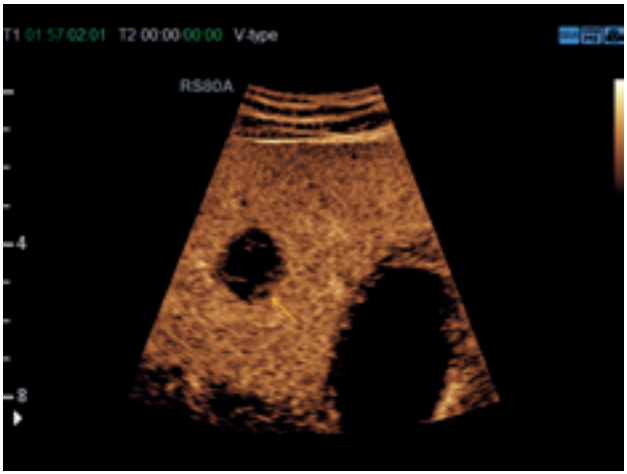

Figure 15: In the **late phase**, the lesion (yellow arrow) stands out from the surrounding liver tissue following intense wash-out. The lesion was confirmed by histology as a liver metastasis originating from a squamous cell carcinoma secondary to a primary pharyngeal carcinoma.

Case review 4

Figure 16: 62-year-old male patient with a small, hypoechoic lesion (yellow arrow).

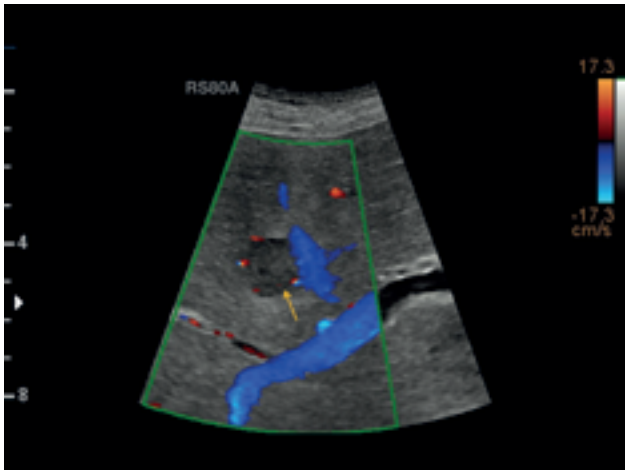

Figure 17: The hypoechoic lesion (yellow arrow) displays increased marginal vascularization in color duplex sonography.

Figure 18: Contrast-enhanced ultrasound. In the **arterial phase**, the lesion is delineated by moderate enhancement (yellow arrow).

Figure 19: In the **portal venous phase**, wash-out of the lesion (yellow arrow) allows it to be distinguished from the surrounding liver tissue.

Figure 20: In the **late phase**, the lesion (yellow arrow) stands out from the surrounding liver tissue following intense wash-out. The lesion was confirmed by histology as a liver metastasis originating from a renal cell carcinoma.

Case review 5

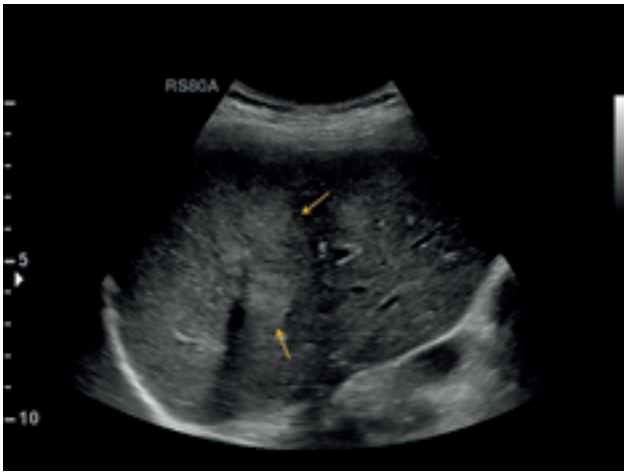

Figure 21: 42-year-old female patient with a suspected large, isoechoic lesion (yellow arrows) in the right lobe of the liver.

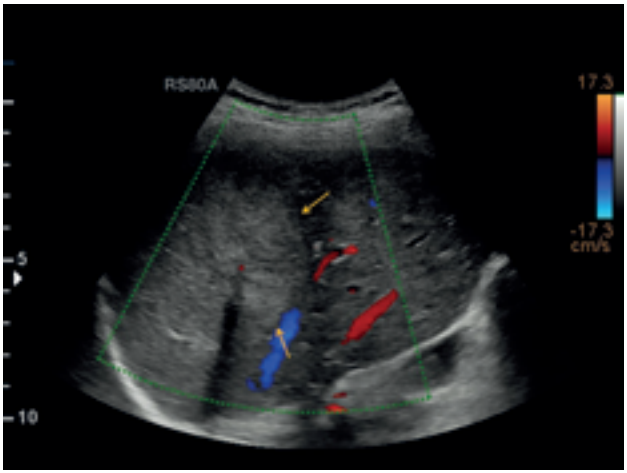

Figure 22: The lesion (yellow arrows) does not display any increase in vascularization in color duplex sonography.

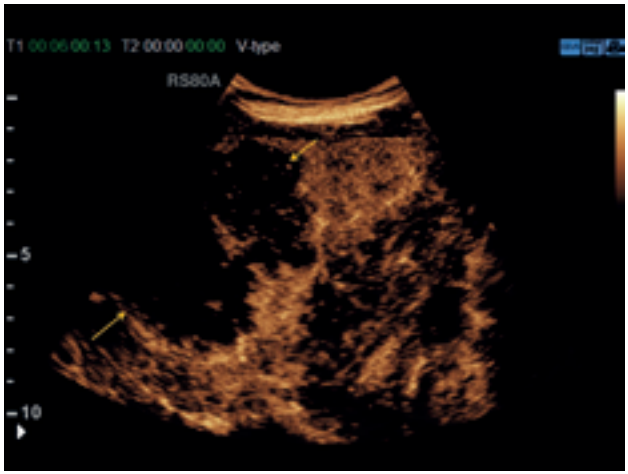

Figure 23: Contrast-enhanced ultrasound. In the **arterial phase**, the lesion is delineated by moderate enhancement (yellow arrows).

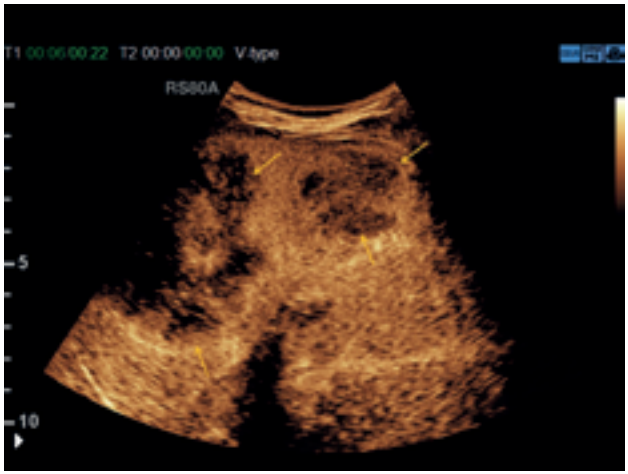

Figure 24: In the **portal venous phase**, wash-out of the two lesions (yellow arrows) allows them to be distinguished from the surrounding liver tissue.

Figure 25: In the **late phase**, the lesions (yellow arrows) stand out from the surrounding liver tissue following intense wash-out. The lesions were confirmed by histology as liver metastases originating from a colorectal carcinoma.

Case review 6

Figure 26: 66-year-old male patient with a hypoechoic lesion (yellow arrow) approx. 2 cm in size.

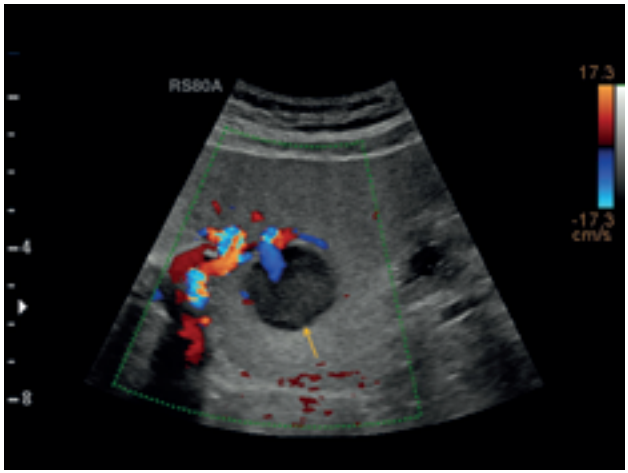

Figure 27: The lesion (yellow arrow) does not display any increase in vascularization in color duplex sonography.

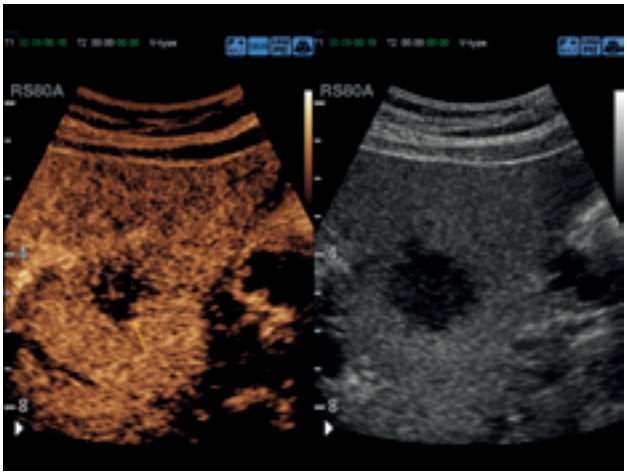

Figure 28: Contrast-enhanced ultrasound. In the **arterial phase**, the lesion is delineated by moderate enhancement (yellow arrow).

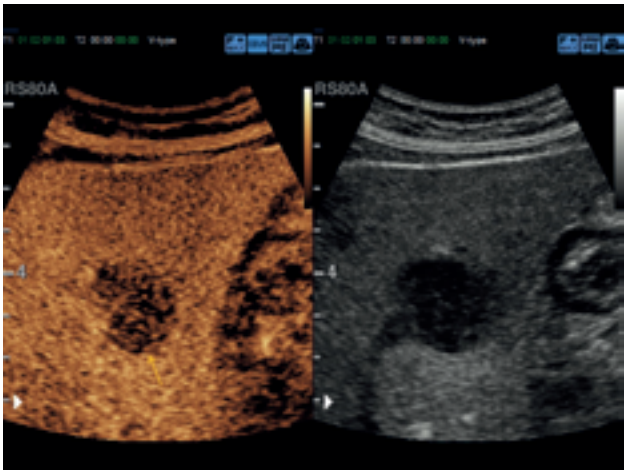

Figure 29: In the **portal venous phase**, wash-out of the lesion (yellow arrow) allows it to be distinguished from the surrounding liver tissue.

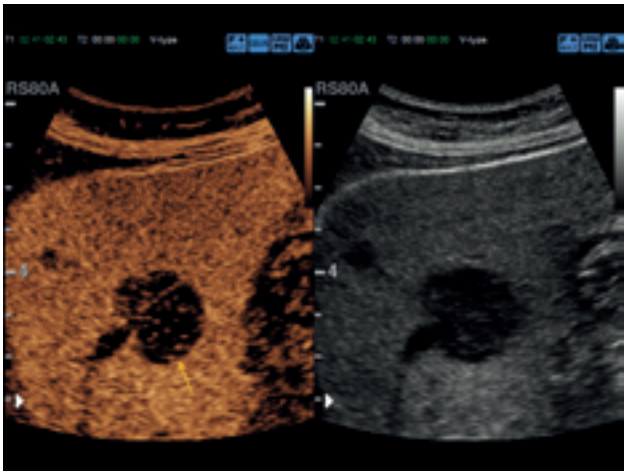

Figure 30: In the **late phase**, the lesion (yellow arrow) stands out from the surrounding liver tissue following intense wash-out. The lesion was confirmed by histology as a liver metastasis originating from a small cell lung carcinoma.

Case review 7

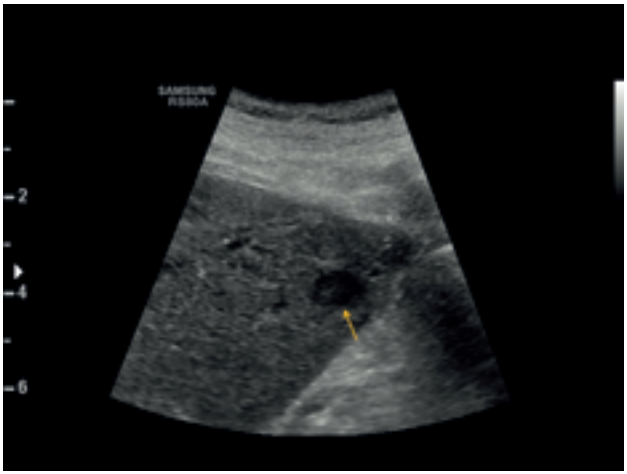

Figure 31: 59-year-old male patient with a hypoechoic lesion (yellow arrow) approx. 1 cm in size.

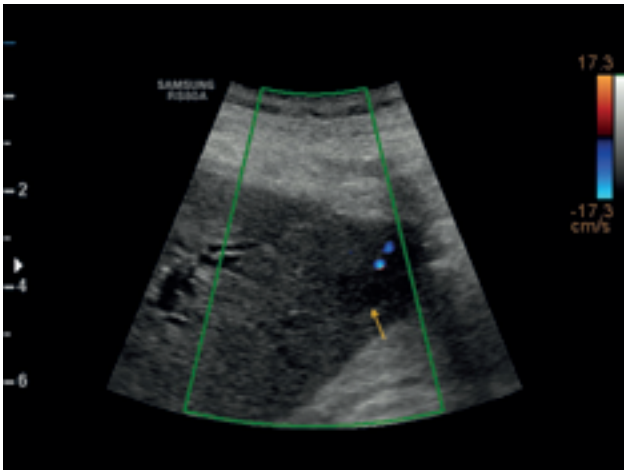

Figure 32: The lesion (yellow arrow) does not display any increase in vascularization in color duplex sonography.

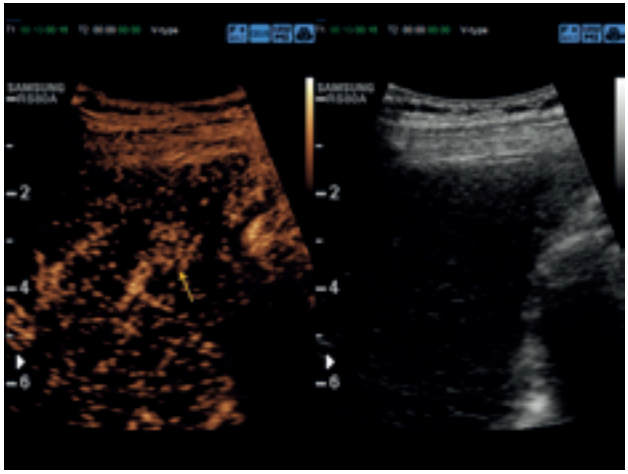

Figure 33: Contrast-enhanced ultrasound. In the **arterial phase**, the lesion is delineated by increased enhancement (yellow arrow).

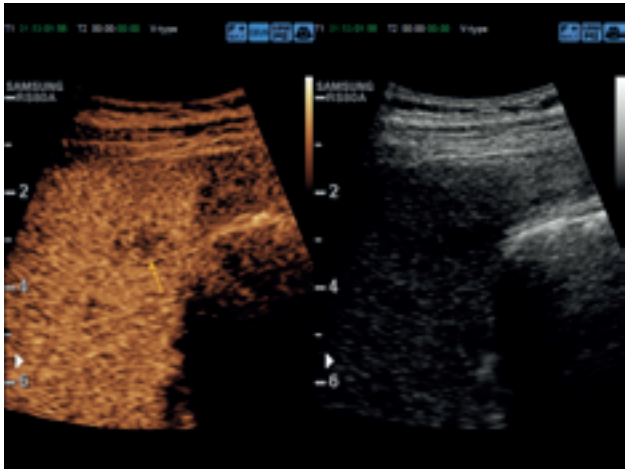

Figure 34: In the **portal venous phase**, wash-out of the lesion (yellow arrow) allows it to be distinguished from the surrounding liver tissue.

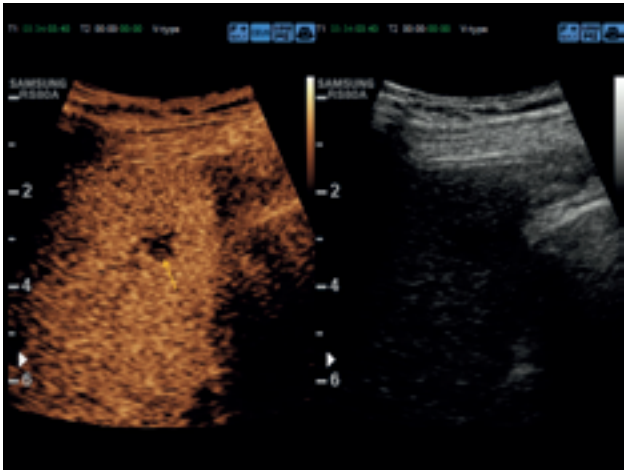

Figure 35: In the **late phase**, the lesion (yellow arrow) stands out from the surrounding liver tissue following wash-out. The lesion was confirmed by histology as a liver metastasis originating from a pancreatic carcinoma.

Case review 8

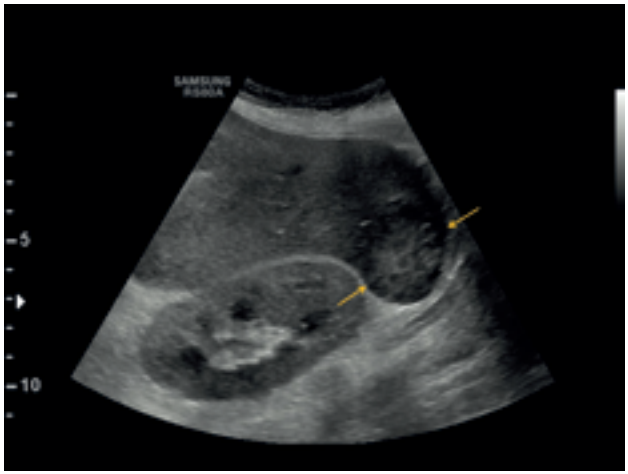

Figure 36: 70-year-old female patient with a mixed hypo-/ hyperechoic lesion (yellow arrows) approx. 3.5 cm in size.

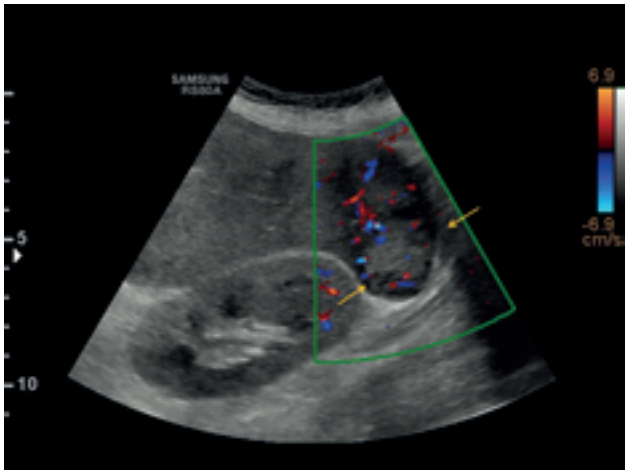

Figure 37: The lesion (yellow arrows) displays increased vascularization in color duplex sonography.

Figure 38: Contrast-enhanced ultrasound. In the **arterial phase**, the lesion is delineated by intense enhancement (yellow arrows).

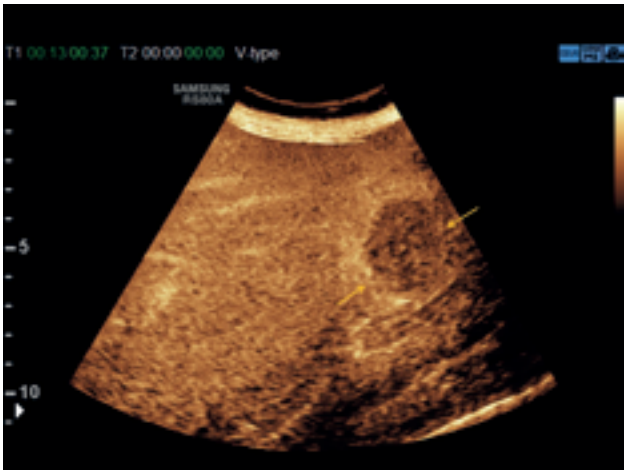

Figure 39: In the **portal venous phase**, wash-out of the lesion (yellow arrows) allows it to be distinguished from the surrounding liver tissue.

Figure 40: In the **late phase**, the lesion (yellow arrows) stands out from the surrounding liver tissue following wash-out. The lesion was confirmed by histology as a liver metastasis originating from a large-cell neuroendocrine carcinoma.

Case review 9

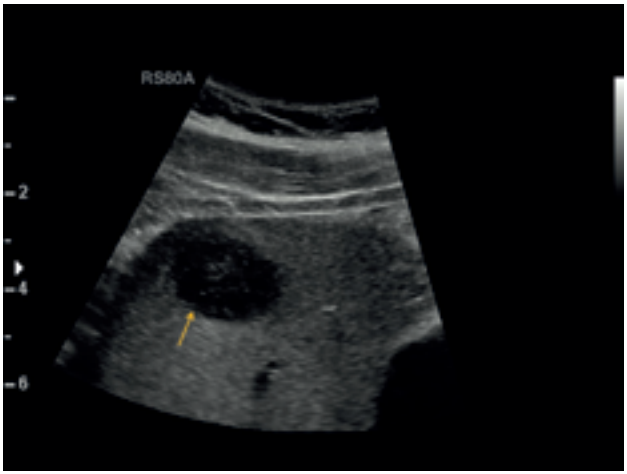

Figure 41: 57-year-old male patient with a hypoechoic lesion (yellow arrow) approx. 2 cm in size.

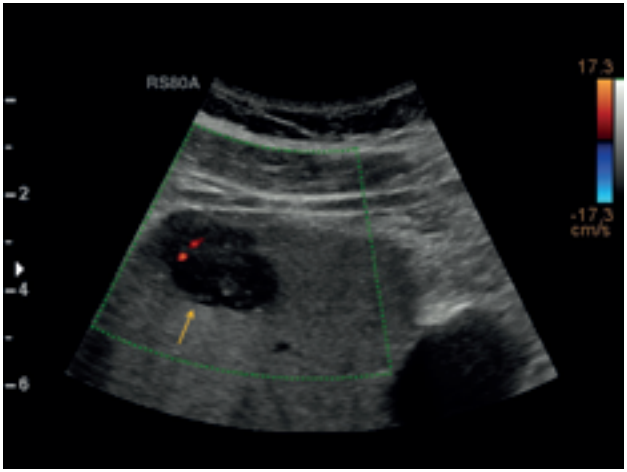

Figure 42: The lesion (yellow arrow) displays increased vascularization in color duplex sonography.

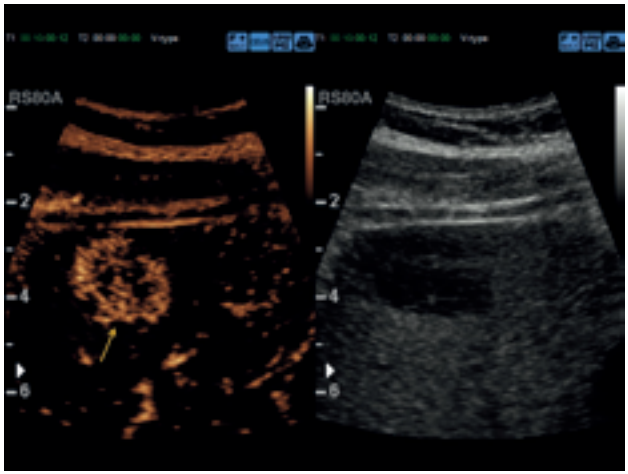

Figure 43: Contrast-enhanced ultrasound. In the **arterial phase**, the lesion is delineated by intense enhancement (yellow arrow).

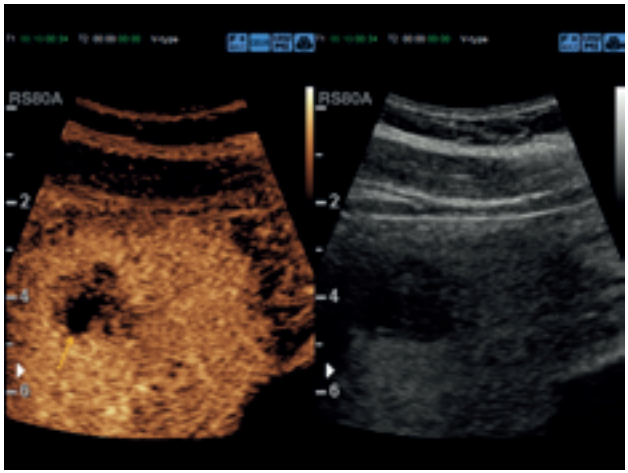

Figure 44: In the **portal venous phase**, wash-out of the lesion (yellow arrow) allows it to be distinguished from the surrounding liver tissue.

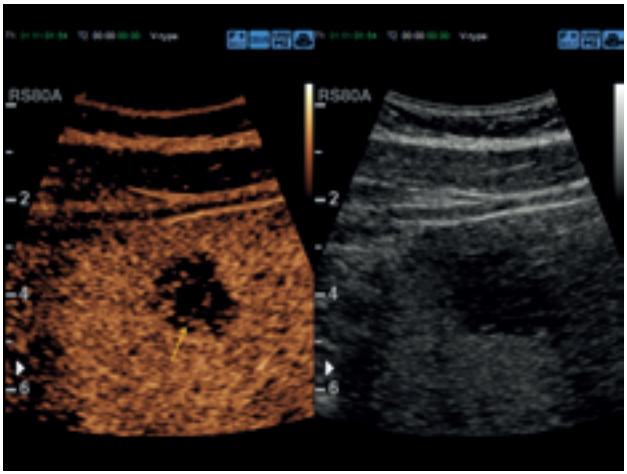

Figure 45: In the **late phase**, the lesion (yellow arrow) stands out from the surrounding liver tissue following wash-out. The lesion was confirmed by histology as a liver metastasis originating from a round cell liposarcoma.

3.2 Lymphoma

Hepatic lymphomas may lead to diffuse, infiltrating lesions as well as to focal lesions in the liver. The appearance of lymphoma may vary between hypoechoic and hyperechoic in B-mode ultrasound. In a study by Trenker et al. investigating 37 patients with hepatic lymphoma, 97.4% of lymphomas were hypoechoic in ultrasound. Hypoechoic liver lesions that do not displace healthy blood vessels in the liver may also be hepatic lymphomas. These may appear as hyperechoic or isoechoic lesions during the arterial phase that are not linked to the portal vein or hepatic veins and are therefore washed out during the portal venous phase [Ochs 2014; Trenker et al. 2014; Weskott 2010] (Figs. 46–50).

3.2.1 Case review – Lymphoma

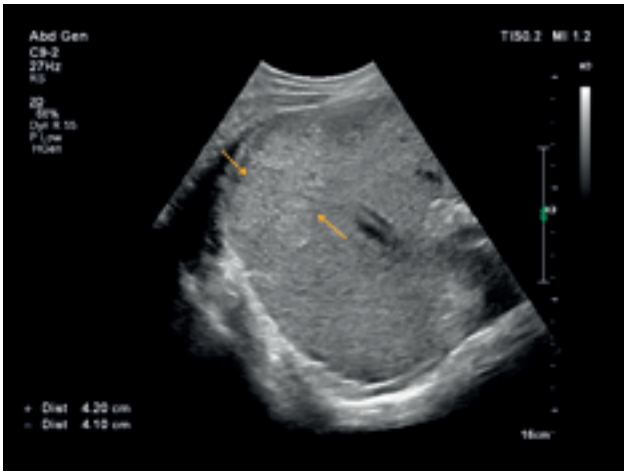

Figure 46: A 34-year-old male patient presented with a liver lesion (yellow arrows) of unknown origin.

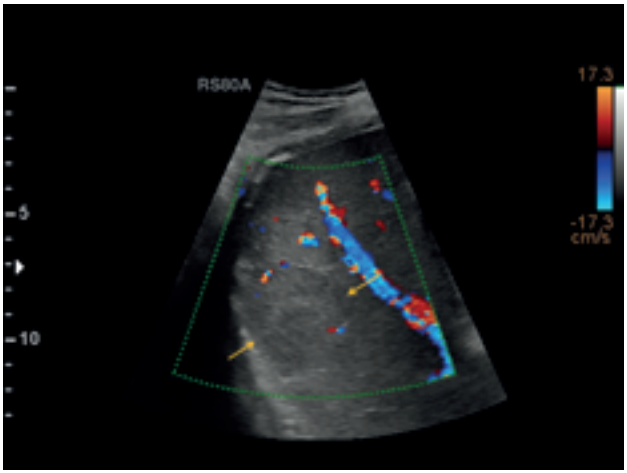

Figure 47: The lesion (yellow arrows) displays increased vascularization in color duplex sonography, and appears hypoechoic at the margins and otherwise isoechoic to the surrounding parenchyma by B-mode imaging.

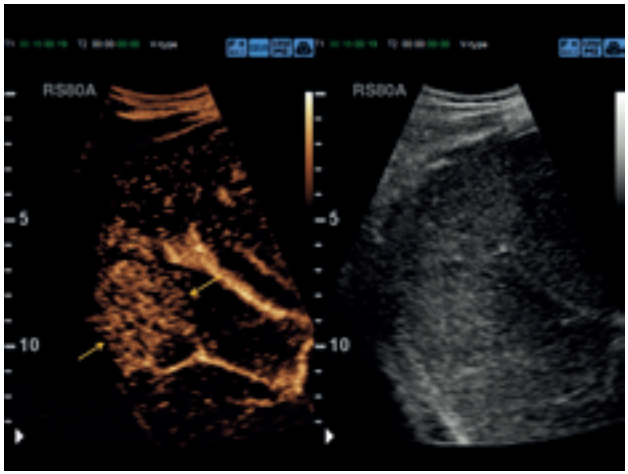

Figure 48: Contrast-enhanced ultrasound. In the **arterial phase**, the lesion is delineated by intense enhancement (yellow arrows).

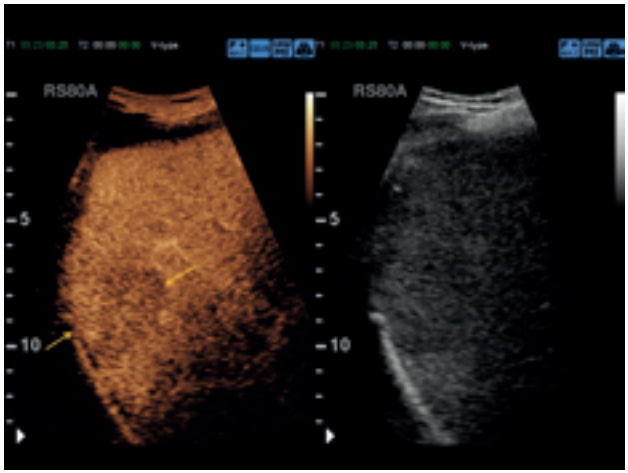

Figure 49: In the **portal venous phase**, wash-out of the lesion (yellow arrows) allows it to be distinguished from the surrounding liver tissue.

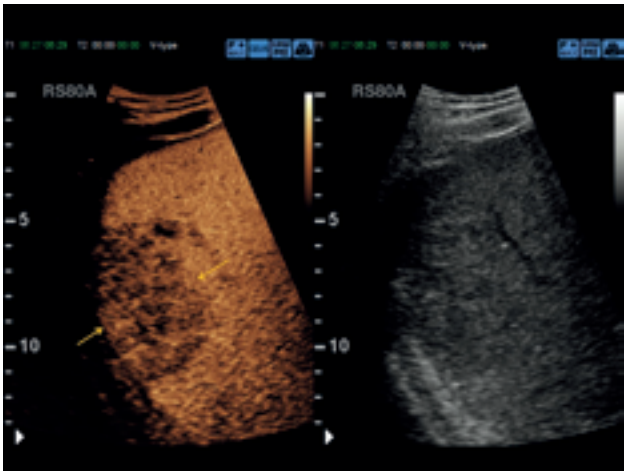

Figure 50: In the **late phase**, the lesion (yellow arrows) stands out from the surrounding liver tissue following wash-out. The diagnosis of hepatic lymphoma was confirmed by histology.

3.3 Hepatocellular carcinoma

Hepatocellular carcinoma (HCC) is the fifth-most common form of cancer worldwide. The incidence of this disease has risen over the past decades and is currently at 10–30 new cases per 100,000 residents per year in Western countries [Bosch et al. 2004]. An estimated 523,000–635,000 people worldwide developed HCC in 2008 [Jemal et al. 2011].

Up to 80% of the global cases of the disease afflict residents of Africa and Southeast Asia, as the high incidence of chronic hepatitis B virus (HBV) infection in these countries promotes the development of HCC. The incidence of HCC is much lower in Europe, North America, and Japan, with an current age-adjusted incidence in Germany of 9.2–10.7 per 100,000 male residents and 1.6–3.6 per 100,000 female residents [Ferlay et al. 2010; S3-Leitlinien [German Guidelines for] HCC 2013].

The groups at high risk of developing HCC are patients with liver cirrhosis of any etiology as well as patients without cirrhosis but with chronic HBV infection or with non-alcoholic fatty liver disease [Bosch et al. 2004; Davila et al. 2005; Marrero et al. 2002; Starley et al. 2010; Welzel et al. 2011]. Nearly 90% of HCC patients in the Western world have liver cirrhosis (affecting up to 4% of cirrhosis patients per year). Accordingly, cirrhosis is considered to be a precancerous condition. The cumulative risk of developing HCC depends on the etiology of the liver disorder, and is greatest among patients with hepatitis B or C virus infection [El-Serag 2011; Güthle & Dollinger 2014].

Approximately 15–20% of HCC patients do not have cirrhosis of the liver (Figs. 51–60). All of the causes of HCC in patients with cirrhosis can also lead to HCC in the absence of cirrhosis. HCC can be roughly classified into **three groups** based on relative incidence:

I. HCC that is rarely developed without cirrhosis (for example in patients with viral hepatitis or alcohol abuse).

II. HCC that is frequently developed even in the absence of cirrhosis (for example in patients with α_1-antitrypsin deficiency, hemochromatosis, non-alcoholic fatty liver disease).

III. HCC that is nearly always developed in the absence of cirrhosis (for example in patients with glycogen storage disease type I, use of oral contraceptives/anabolic steroids) [Evert & Dombrowski 2008].

HCC can manifest as diffuse, focal, or pedunculated forms. Its morphology is highly variable when viewed by ultrasound, and a single nodule may often contain multiple intensities with both hypoechoic and hyperechoic regions.

It is often difficult to distinguish HCC by B-mode ultrasound in a cirrhotic liver with large nodules, and it does not always appear hypervascular by color Doppler in this situation. Following administration of contrast agent, HCC typically displays intense enhancement that is usually associated with a chaotic vascular pattern. This enhancement becomes isoechoic with the surrounding parenchyma during the portal venous phase and is eventually washed out during the late phase (Figs. 61–70). However, the enhancement pattern of well-differentiated HCC may deviate from this description. This form of HCC displays intense arterial enhancement which then diminishes to the level of the surrounding parenchyma but is not clearly washed out during the late phase. Therefore, well-differentiated HCC must be considered a possibility when a lesion with arterial enhancement and no wash-out is detected in a cirrhotic liver [Claudon et al. 2013; Nicolau et al. 2006]. Nonetheless, there is often no hyper-enhancement of well-differentiated HCC during the arterial phase [Choi et al. 2015; Shah et al. 2014]. Finally, 10% of HCCs are primary hypovascular in CEUS [Boozari et al. 2011; Schellhaas et al. 2016] (Tables 7 and 8).

In a multicenter study in Germany, CEUS could successfully characterize HCC with a sensitivity of 86.1% and a specificity of 96.6%, compared with a sensitivity of 69.4% and a specificity of 95.1% for spiral CT. This study also demonstrated that the use of CEUS could reduce the number of liver biopsies performed [Strobel et al. 2008]. In patients with liver cirrhosis, it is often necessary to combine different ultrasound techniques – especially CEUS – to enable differentiation between regenerative or dysplastic lesions and malignant lesions [Jung et al. 2012]. In addition to characterizing focal liver lesions, CEUS may also provide additional information that may prove useful for selecting the most appropriate form of treatment. Liver metastases and HCC can be treated by surgery, liver-directed procedures, or other therapies [Müller-Peltzer et al. 2017].

Lesion	Arterial phase	Portal venous phase	Late phase
Non-cirrhotic liver			
HCC			
Typical signs	Hyper-enhancement	Iso-enhancement	Hypo-enhancement to non-enhancement
Other findings	Regions without enhancement	Regions without enhancement	Regions without enhancement

Table 7: Enhancement patterns of hepatocellular carcinoma (HCC) in a non-cirrhotic liver [Claudon et al. 2013].

Lesion	Arterial phase	Portal venous phase	Late phase
Cirrhotic liver			
HCC			
Typical signs	Complete hyper-enhancement	Iso-enhancement	Hypo-enhancement (mild to moderate)
	For large tumors: Regions without enhancement possible	Regions without enhancement	
Other findings	Basket-like pattern, chaotic vascular pattern		
	Malignant thrombus with enhancement		Iso-enhancement
	Hypo-enhance-ment to non-enhancement	Non-enhancement	Non-enhancement

Table 8: Enhancement patterns of hepatocellular carcinoma (HCC) in a cirrhotic liver [Claudon et al. 2013].

3.3.1 Case reviews – Hepatocellular carcinoma

Case review 1

Figure 51: 67-year-old male patient with a hypoechoic lesion (yellow arrow) of unknown origin in a non-cirrhotic liver.

Figure 52: The hypoechoic lesion (yellow arrow) does not display any increase in vascularization in color duplex sonography.

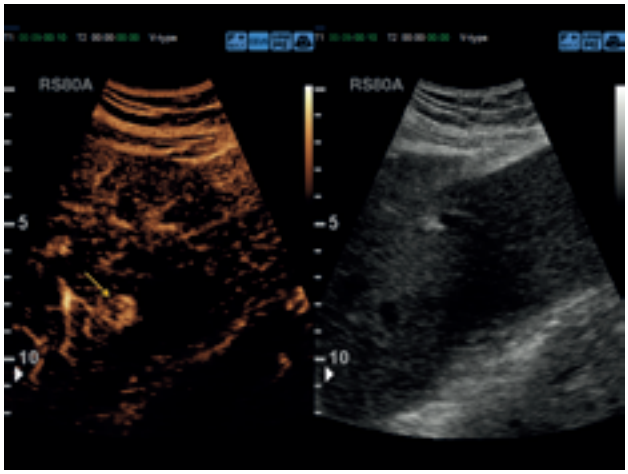

Figure 53: Contrast-enhanced ultrasound. Examined by dual-image display (CEUS and B-mode display). In the **arterial phase**, the lesion is delineated by intense enhancement (yellow arrow).

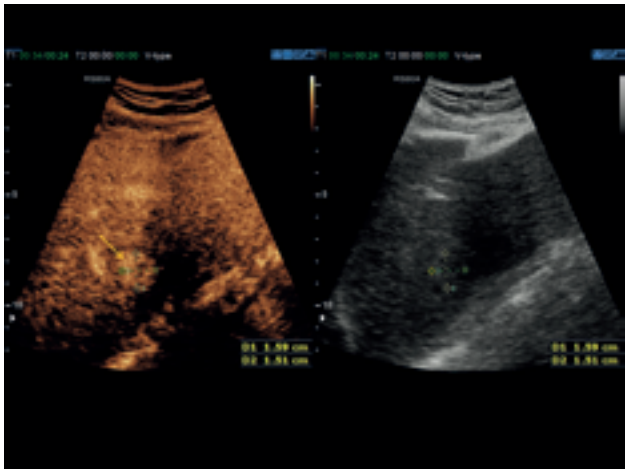

Figure 54: In the **portal venous phase** after 30 seconds, the enhancement within the lesion (yellow arrow) becomes somewhat more delineated from the surrounding liver tissue, but there is no wash-out of the lesion.

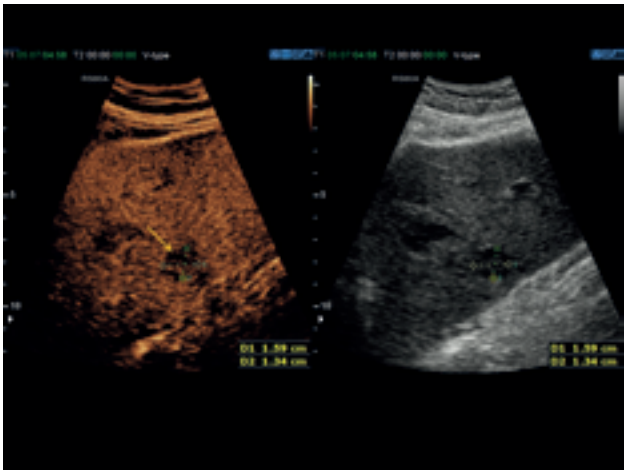

Figure 55: In the **late phase** after 5 minutes, the lesion (yellow arrow) becomes visible against the surrounding liver tissue following wash-out. The lesion was confirmed by histology as a moderately differentiated hepatocellular carcinoma in a non-cirrhotic liver.

Case review 2

Figure 56: 66-year-old male patient with large, central liver lesion (yellow arrows) in a non-cirrhotic liver. A CT performed at another facility led to a diagnosis of hemangioma. Adjunct contrast-enhanced ultrasound was then performed due to elevated levels of alpha-fetoprotein of 118 ng/ml.

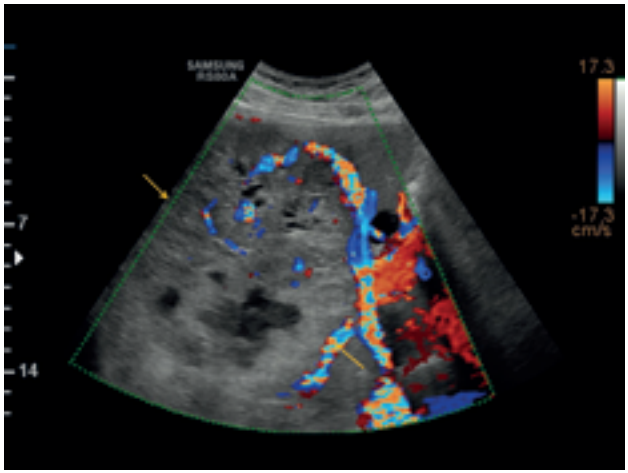

Figure 57: The suspected lesion (yellow arrows) displays increased vascularization in color duplex sonography.

Figure 58: Contrast-enhanced ultrasound. In the **arterial phase**, the lesion is delineated by intense, basket-like enhancement (yellow arrows).

Figure 59: In the **portal venous phase** after approx. 30 seconds, the enhancement within the lesion (yellow arrows) becomes somewhat more delineated from the surrounding liver tissue, but there is no wash-out of the lesion. The central regions of the lesion display no uptake of contrast agent.

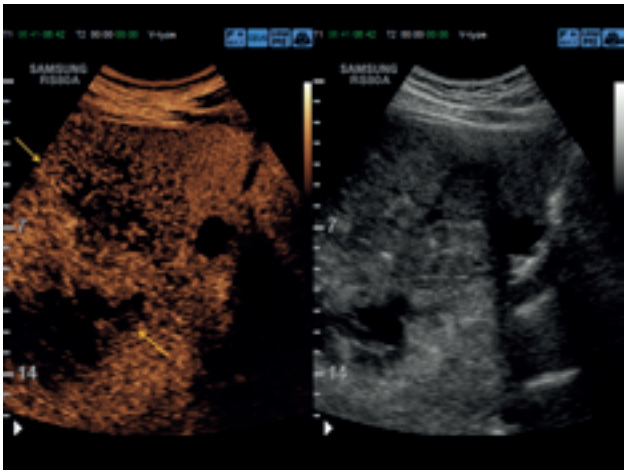

Figure 60: In the **late phase** after over 6 minutes, the lesion (yellow arrows) stands out from the surrounding liver tissue following wash-out. A moderately differentiated hepatocellular carcinoma was confirmed by histology with no evidence of extensive fibrosis or cirrhotic remodeling of the liver. No adequate evidence pointing to fibrolamellar hepatocellular carcinoma was provided by histomorphology and immunohistochemistry.

Case review 3

Figure 61: 53-year-old female patient with known cirrhosis and concurrent ascites. During the admission examination, a nearly isoechoic lesion (yellow arrow) approx. 2 cm in size was observed in contact with the gallbladder bed.

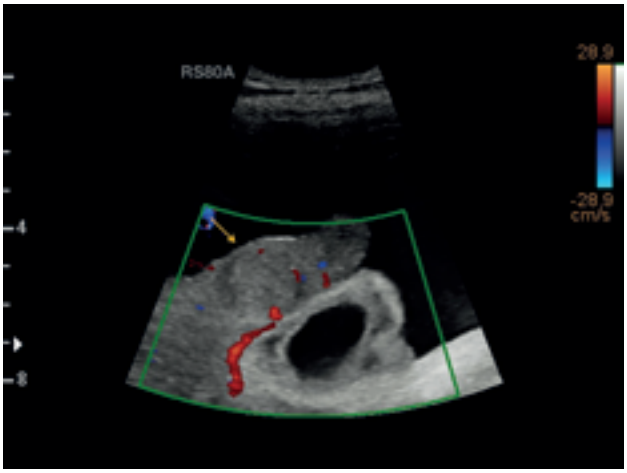

Figure 62: The suspected lesion (yellow arrow) displays increased discrete vascularization in color duplex sonography.

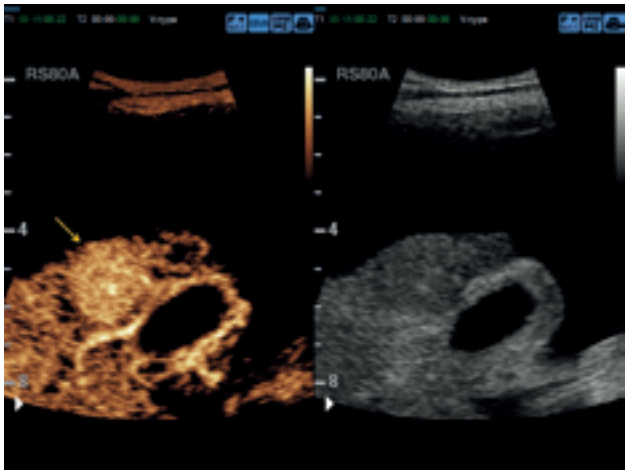

Figure 63: Contrast-enhanced ultrasound. Examined by dual-image display (CEUS and B-mode display). In the **arterial phase**, the lesion is delineated by intense, homogeneous enhancement (yellow arrow).

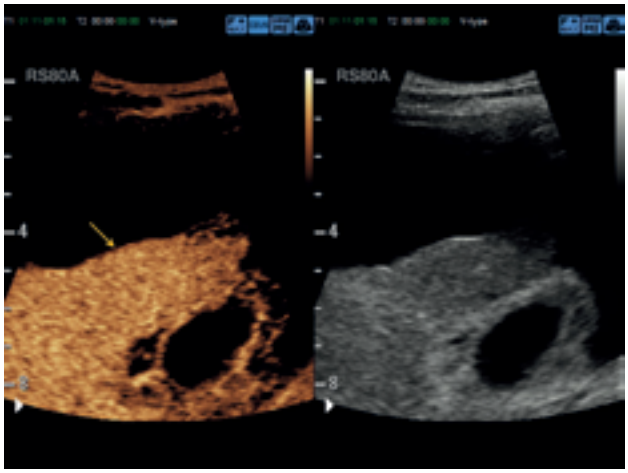

Figure 64: In the **portal venous phase** after 110 seconds, the isoechoic enhancement within the lesion (yellow arrow) becomes somewhat delineated from the surrounding liver tissue, but there is no wash-out of the lesion.

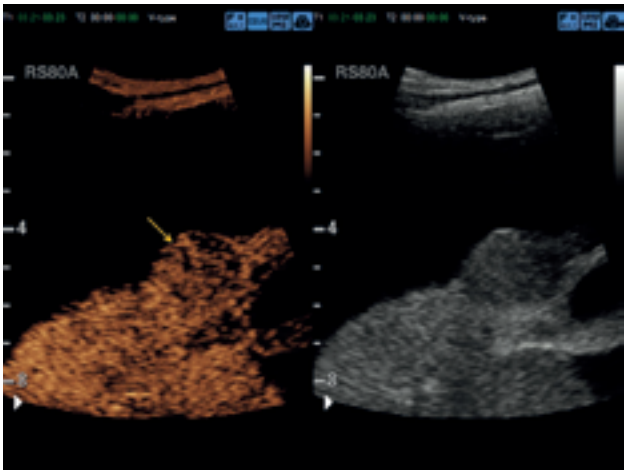

Figure 65: In the **late phase** after over 3 minutes, the lesion (yellow arrow) stands out from the surrounding liver tissue following wash-out. Taking these findings together leads to the conclusion that this lesion is a hepatocellular carcinoma in a cirrhotic liver.

Case review 4

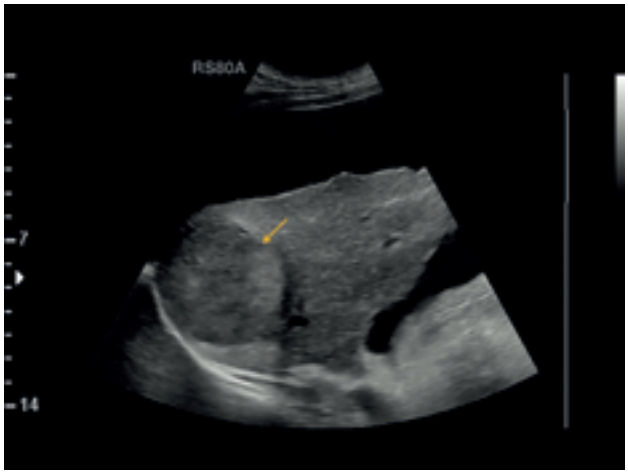

Figure 66: The patient was a 53-year-old female with known cirrhosis and concurrent ascites. A nearly isoechoic lesion approx. 5 cm in size (yellow arrow) is visible.

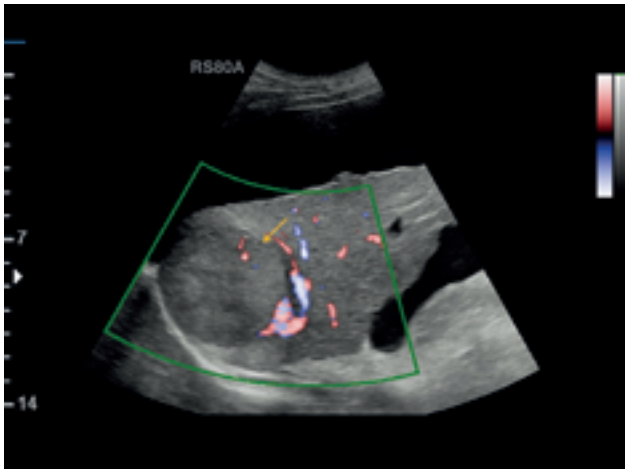

Figure 67: The suspected lesion (yellow arrow) does not display any increase in vascularization in power Doppler ultrasound.

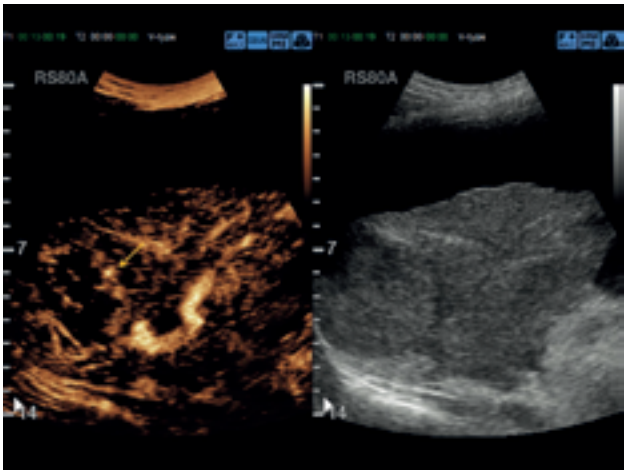

Figure 68: Contrast-enhanced ultrasound. Examined by dual-image display (CEUS and B-mode display). In the **arterial phase**, the lesion is delineated by intense marginal enhancement (yellow arrow).

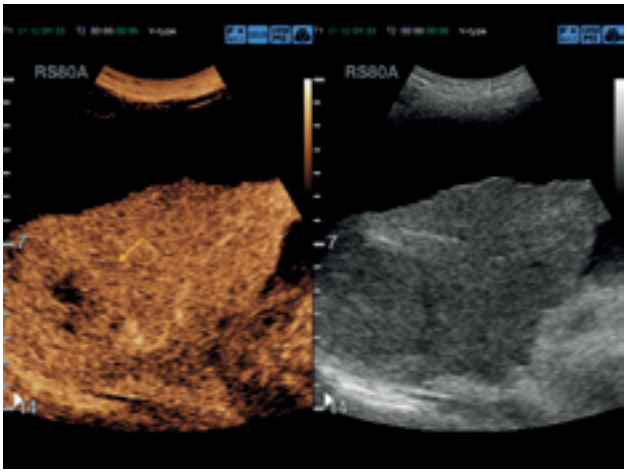

Figure 69: In the **portal venous phase** after approx. 90 seconds, the isoechoic enhancement within the lesion (yellow arrow) becomes somewhat delineated from the surrounding liver tissue. The central regions of the lesion display no uptake of contrast agent.

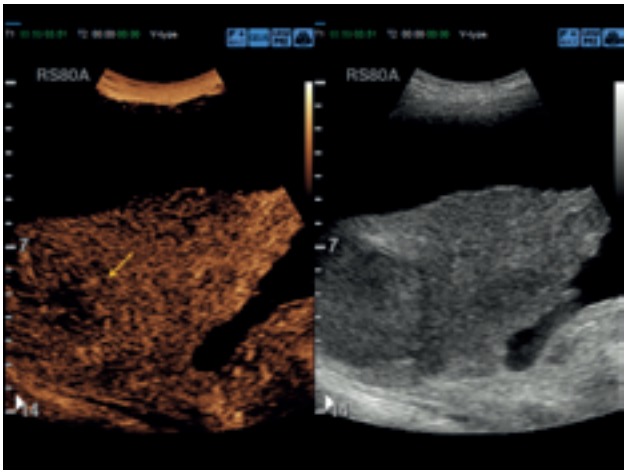

Figure 70: In the **late phase** after nearly 4 minutes, the lesion (yellow arrow) becomes visible against the surrounding liver tissue following discrete wash-out. Taking these findings together leads to the conclusion that this lesion is a hepatocellular carcinoma in a cirrhotic liver.

3.4 Fibrolamellar hepatocellular carcinoma

Fibrolamellar hepatocellular carcinoma (FHCC) is a variant of hepatocellular carcinoma (HCC) with several unique clinical and histopathological characteristics. FHCC represents less than 3% of all cases of HCC, and unlike HCC it typically afflicts non-cirrhotic livers and younger patients (5–35 years old) (Figs. 71–75). FHCC has a favorable prognosis when resectable, with a mean survival of 32 months following diagnosis [Craig et al. 1980; Epstein et al. 1999; McLarney et al. 1999].

The histology of FHCC is characterized by eosinophilic hepatocyte neoplasms arranged in laminated layers located in dense collagenous connective tissue [Spangenberg et al. 2007].

3.4.1 Case review – Fibrolamellar hepatocellular carcinoma

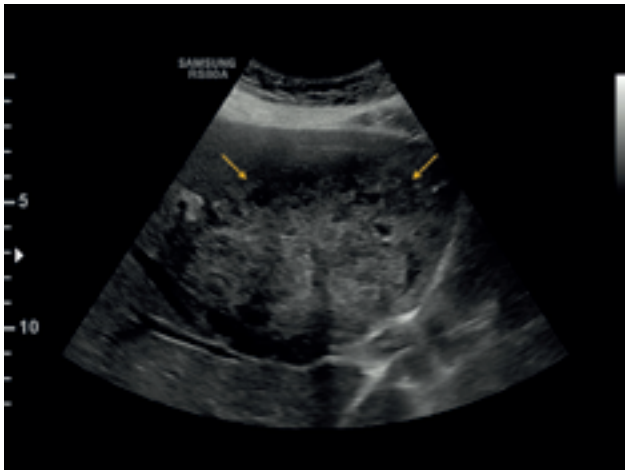

Figure 71: 36-year-old female patient with large, central liver lesion (yellow arrows) in a non-cirrhotic liver.

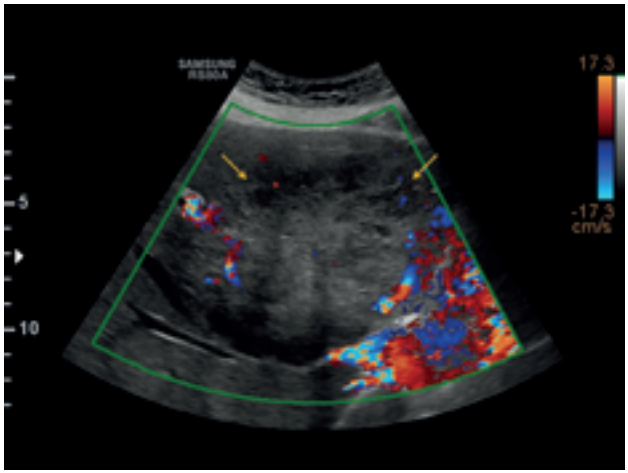

Figure 72: The suspected lesion (yellow arrows) displays increased marginal vascularization in color duplex sonography.

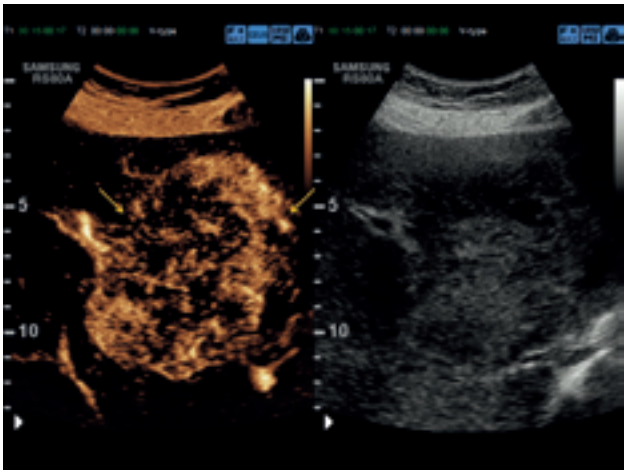

Figure 73: Contrast-enhanced ultrasound. Examined by dual-image display (CEUS and B-mode display). In the **arterial phase**, the lesion is delineated from the surrounding parenchyma by intense enhancement (yellow arrows).

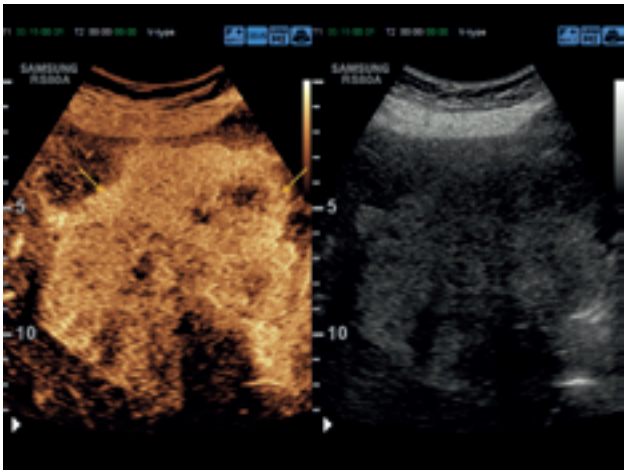

Figure 74: In the **portal venous phase** after approx. 30 seconds, the enhancement within the lesion (yellow arrows) becomes more delineated from the surrounding liver tissue.

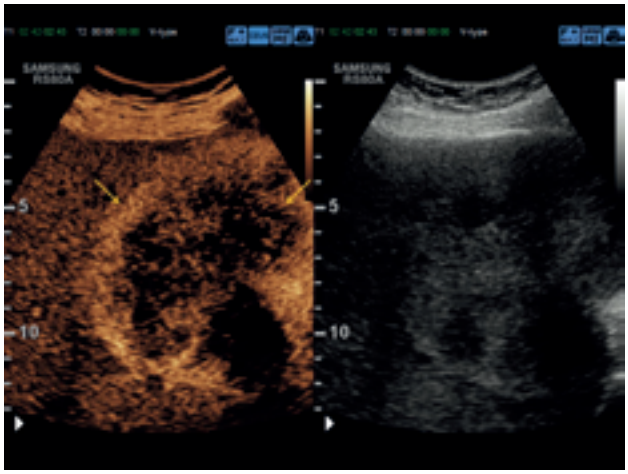

Figure 75: In the **late phase** after over 2 minutes and 40 seconds, the lesion (yellow arrows) stands out from the surrounding liver tissue following wash-out primarily in its center. The lesion was confirmed by histology as a moderately-differentiated fibrolamellar hepatocellular carcinoma. Alpha-fetoprotein levels were normal at 2 ng/ml.

3.5 Cholangiocarcinoma

While the most prevalent form of primary malignant liver tumor is hepatocellular carcinoma (HCC), cholangiocarcinoma (CCC) is the second-most prevalent form of malignant liver lesion. CCC can be intrahepatic or peripheral in the parenchyma of the liver, with these two forms together comprising about 15% of all primary hepatobiliary malignancies. CCC, or bile duct cancer, is a relatively rare form of biliary tumor with an incidence of 0.4–1.3 per 100,000 residents per year [Samaras et al. 2011].

CCC is an epithelial tumor that spreads through the bile ducts and displays the typical histological characteristics of differentiated cholangiocytes [Rizvi & Gores 2013; Vogel et al. 2014].

A study by Blechacz and Gores demonstrated that CCC arises from a malignant transformation of cholangiocytes in the intrahepatic bile ducts [Blechacz & Gores 2008a].

Patients both with and without liver cirrhosis can develop CCC [Kobayashi et al. 2000; Wengert et al. 2015; Zhou et al. 2009].

There has recently been an increase in the incidence of peripheral CCC, although no pathogenic explanation has been postulated to date [Poultsides et al. 2010].

CCC frequently has a poor prognosis. This is because patients typically present nonspecific clinical symptoms during the early stages of the disease, and as a result many tumors are not detected until the advanced stage. The long-term survival rate of CCC is only 20–30% [Nagorney et al. 1993].

Without treatment, patients with unresectable CCC have a 1-year survival rate of about 25% and a 5-year survival rate of 3%. The mean survival time of these patients is 6–8 months [Harder 2009].

The carcinogenesis of this form of malignancy involves chronic inflammation, cholestasis, and other risk factors. Table 9 lists the risk factors for developing CCC.

CCCs can be subdivided into intrahepatic and extrahepatic tumors based on their anatomical localization. Approximately 10% of intrahepatic tumors have a peripheral localization. The extrahepatic tumors can be further subdivided into distal extrahepatic tumors (30%) and the more common perihilar form (Klatskin tumor, 50–60%) [Weskott 2010].

Klatskin tumors are classified based on hepatic duct involvement (Bismuth-Corlette stages I–IV; Table 10) [Bismuth et al. 1992; Nakeeb et al. 1996].

The introduction of modern, high-resolution systems has greatly improved the sensitivity of ultrasound for the detection and characterization of CCCs and the evaluation of their suitability for resection [Rubens 2007] (Figs. 76–90).

Peripheral CCC typically appears as a lobular, polycystic, moderately hyperechoic mass with poorly-defined margins that is partially surrounded by a hypoechoic halo. The presence of satellite lesions is suggestive of an advanced stage of the disease (Figs. 91–97). Partial hepatic capsular retraction may be due to the atrophy of certain liver segments or to parenchymal fibrosis [Bloom et al. 1999; Claudon et al. 2013; Wermke 2006; Weskott 2010].

It is difficult to assess the vascular architecture of CCC using conventional color Doppler or power Doppler ultrasound.

In contrast, the use of ultrasound contrast agents can overcome these hurdles by revealing microvessels that typically appear very dense during the arterial phase with peripheral, circumferential, rim-like enhancement [Weskott 2010]. Arteries with chaotic or atypical structures and centripetal flow may also be observed. The absence of contrast enhancement in the center of the lesion may indicate deficient intra-tumoral perfusion. CCC may exhibit a very heterogeneous appearance depending on the degree of fibrosis and degeneration [Chen et al. 2008, 2010; D'Onofrio et al. 2008; Wermke 2006]. The enhancement patterns of CCC are listed in Table 11.

CCC starts to become prominent during the portal venous phase and is enhanced in the late phase [Meacock et al. 2010; Xu et al. 2006].

Gallbladder carcinoma is the most common type of cancer of the biliary system and frequently (75%) metastasizes beyond the gallbladder [Wang et al. 2016; Zajaczek et al. 2005]. While it is difficult to diagnose this condition early due to its non-specific symptoms, the use of CEUS in the gallbladder can enable differentiation between "tumorous sludge" and a gallbladder tumor (Figs. 98–101).

Autoimmune disorders:
– Primary sclerosing cholangitis (PSC)
Parasitic causes:
– Asian liver flukes (Opisthorchis viverrini und Clonorchis sinensis)
Viral causes:
– Hepatitis B – Hepatitis C
Malformations:
– Caroli disease – Choledochal cysts – Congenital hepatic fibrosis
Toxic factors:
– Alcohol – Smoking – Nitrosamines – Radiocontrast agents

Table 9: Risk factors for the development of cholangiocarcinoma [Blechacz & Gores 2008b; Claessen et al. 2009; Khan et al. 2005; Shaib & El-Serag 2004].

Bismuth-Corlette staging of perihilar (Klatskin) tumors	
Stage	**Characteristics**
I	Hilar tumor below the confluence of the right and left hepatic ducts
II	Hilar tumor involving the confluence of the right and left hepatic ducts
IIIa	Hilar tumor extending into the right hepatic duct
IIIb	Hilar tumor extending into the left hepatic duct
IV	Hilar tumor extending into both hepatic ducts

Table 10: Staging of Klatskin tumors [Harder 2009].

Lesion	Arterial phase	Portal venous phase	Late phase
Typical signs	Halo-like hyper-enhancement, central hypo-enhancement	Hypo-enhancement	Non-enhancement
Other findings	Regions without enhancement, heterogeneous hyper-enhancement	Regions without enhancement	Regions without enhancement

Table 11: Enhancement patterns of cholangiocarcinoma [Claudon et al. 2013; Wildner et al. 2015].

3.5.1 Case reviews – Cholangiocarcinoma

Case review 1

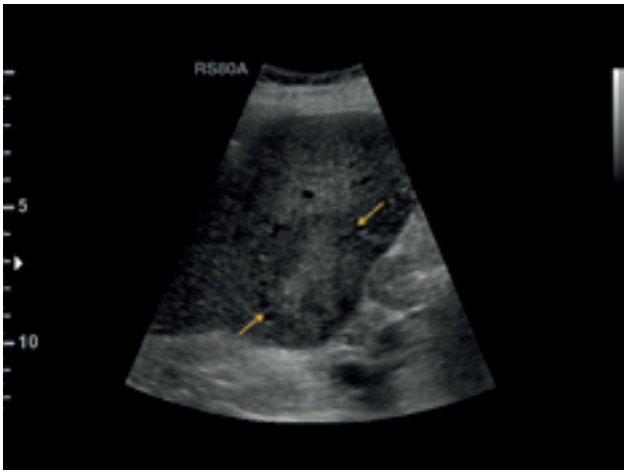

Figure 76: 61-year-old female patient with an intrahepatic lesion (yellow arrows).

Figure 77: The lesion (yellow arrows) does not display any increase in vascularization in color duplex sonography.

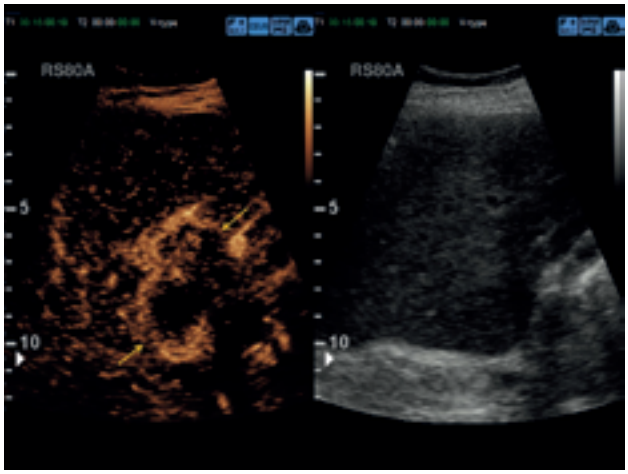

Figure 78: Contrast-enhanced ultrasound. In the **arterial phase**, the lesion is delineated by intense marginal enhancement (yellow arrows).

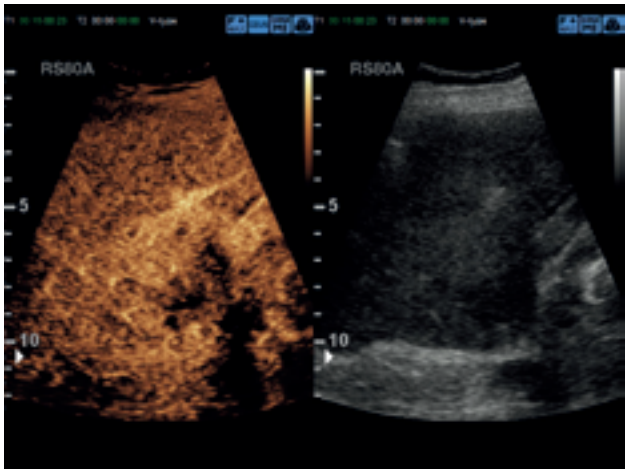

Figure 79: Contrast-enhanced ultrasound. In the somewhat delayed **arterial phase**, this lesion is delineated with slightly reduced central enhancement.

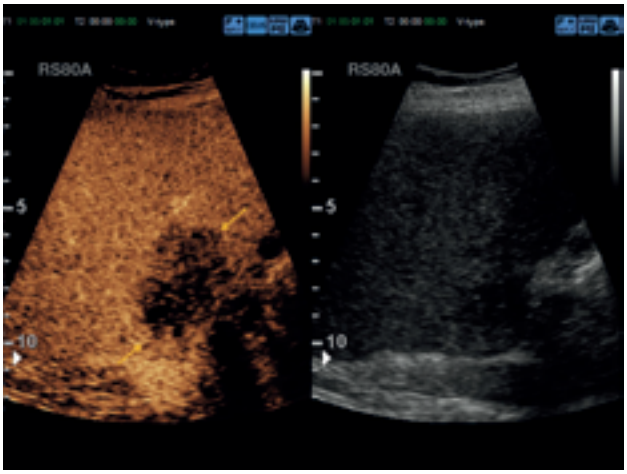

Figure 80: In the **portal venous phase** after approx. 1 minute, wash-out of the lesion (yellow arrows) already allows it to be distinguished from the surrounding liver tissue.

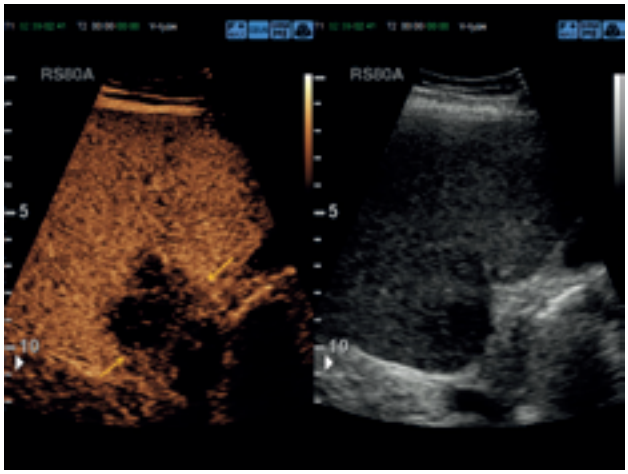

Figure 81: In the **late phase** after approx. 2:30 minutes, wash-out of the lesion (yellow arrows) allows it to be increasingly distinguished from the surrounding liver tissue.

Robust expression of cytokeratin (CK)19 with co-expression of CK7 was observed on atypical glands by immunohistochemistry, together with weak expression of CK20. These immunohistochemistry findings are consistent with cholangiocarcinoma.

Case review 2

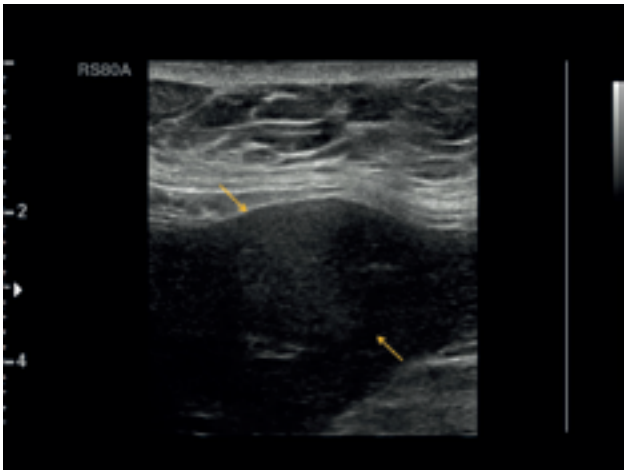

Figure 82: 67-year-old male patient with a peripheral lesion (yellow arrows). A linear probe was used for the examination.

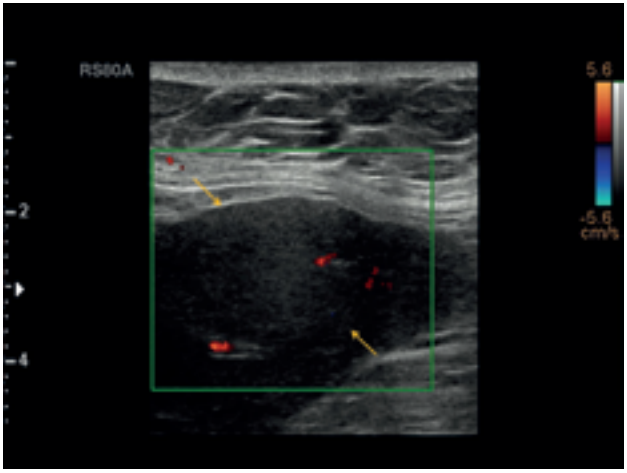

Figure 83: The lesion (yellow arrows) does not display any increase in vascularization in color duplex sonography.

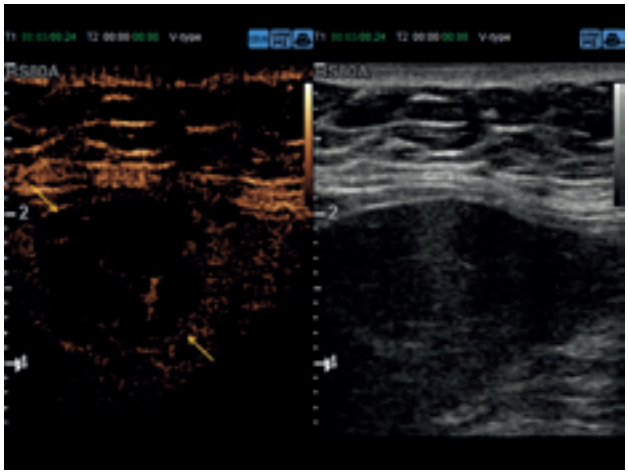

Figure 84: Contrast-enhanced ultrasound. In the **arterial phase**, the lesion is delineated by slight enhancement (yellow arrows).

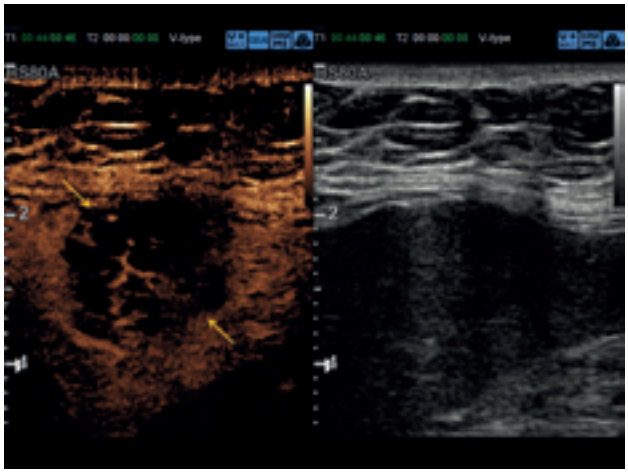

Figure 85: In the **portal venous phase**, the lesion (yellow arrows) can be more easily distinguished from the surrounding liver tissue. This lesion represents peripheral cholangiocarcinoma.

Case review 3

Figure 86: 67-year-old female patient with a suspected intrahepatic, hyperechoic lesion associated with a marginal, hypoechoic halo (yellow arrows) that appears adjacent to the gallbladder bed.

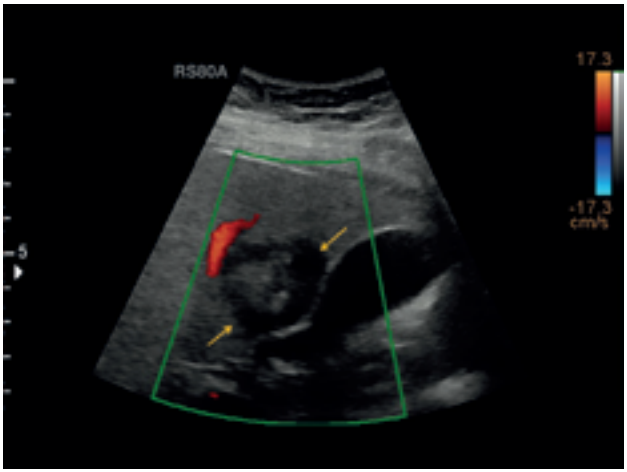

Figure 87: The lesion (yellow arrows) does not display any increase in vascularization in color duplex sonography.

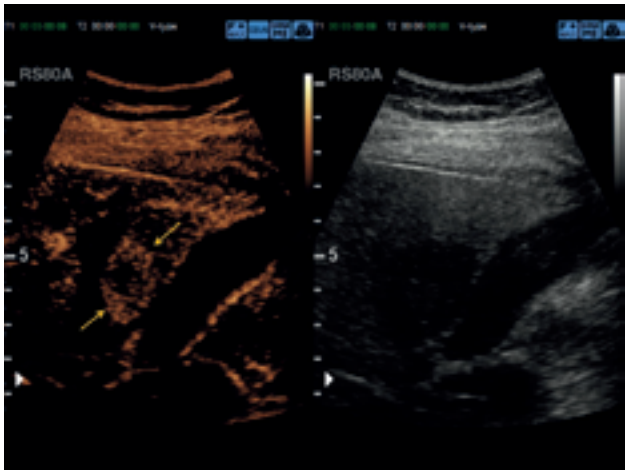

Figure 88: Contrast-enhanced ultrasound. In the **arterial phase**, the lesion (yellow arrows) is delineated by moderate enhancement.

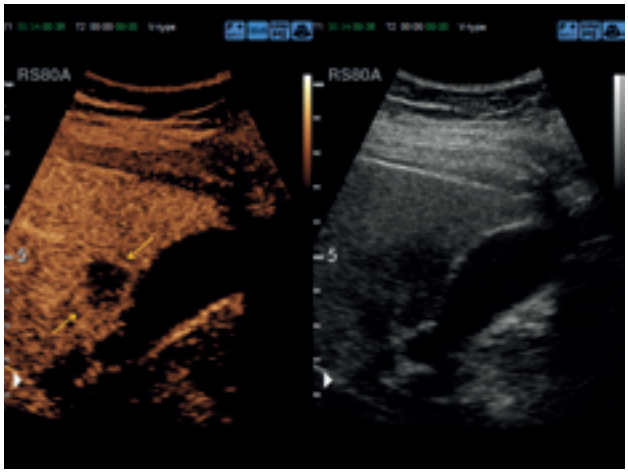

Figure 89: In the **portal venous phase** after approx. 40 seconds, wash-out of the lesion (yellow arrows) already allows it to be distinguished from the surrounding liver tissue.

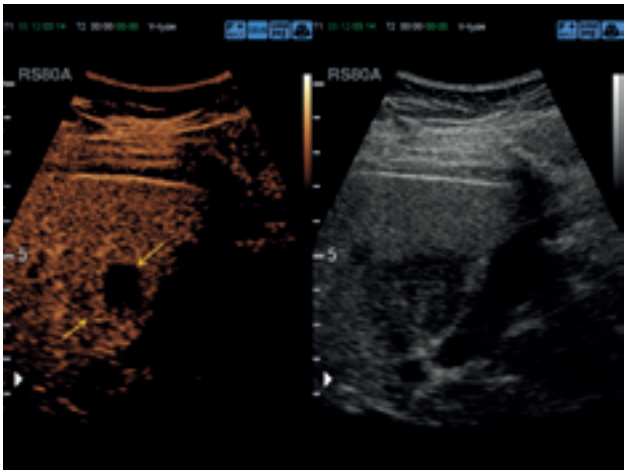

Figure 90: In the **late phase** after approx. 3:10 minutes, wash-out of the lesion (yellow arrows) allows it to be increasingly distinguished from the surrounding liver tissue. Cholangiocarcinoma was confirmed by histology.

Case review 4

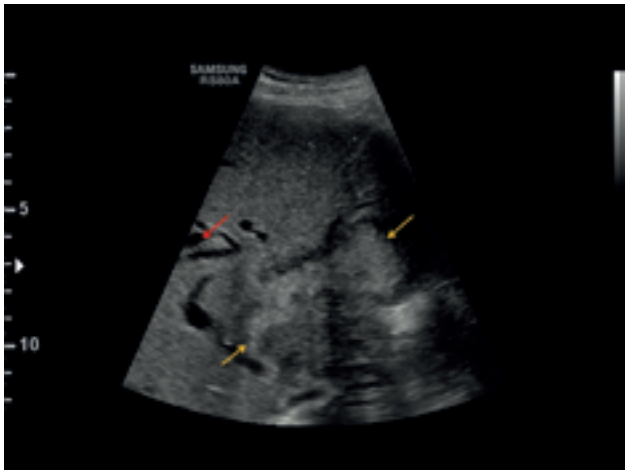

Figure 91: 74-year-old male patient with a suspected large intrahepatic lesion with a marginal hypoechoic halo (yellow arrows) and resulting expansion of a bile duct (red arrow).

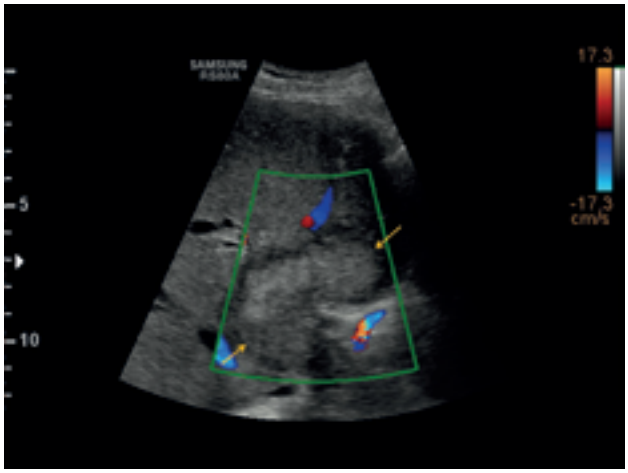

Figure 92: The lesion (yellow arrows) does not display any increase in vascularization in color duplex sonography.

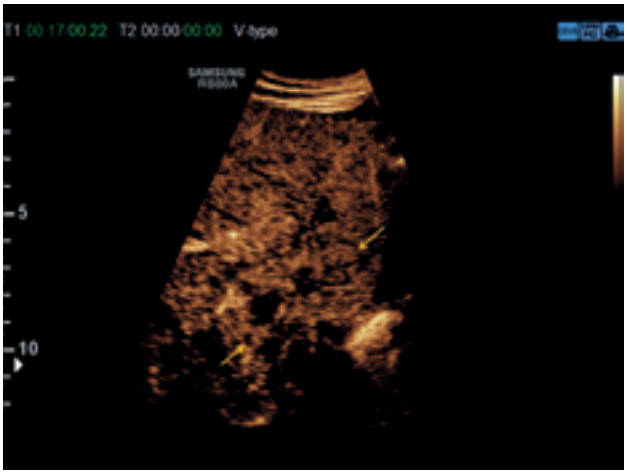

Figure 93: Contrast-enhanced ultrasound. In the **arterial phase**, the lesion is delineated by moderate enhancement.

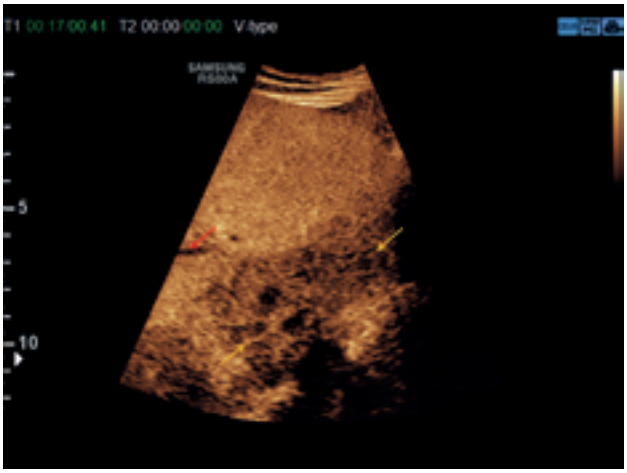

Figure 94: In the **portal venous phase** after approx. 40 seconds, wash-out of the lesion (yellow arrows) already allows it to be distinguished from the surrounding liver tissue. The expansion of a bile duct (red arrow) is also visible.

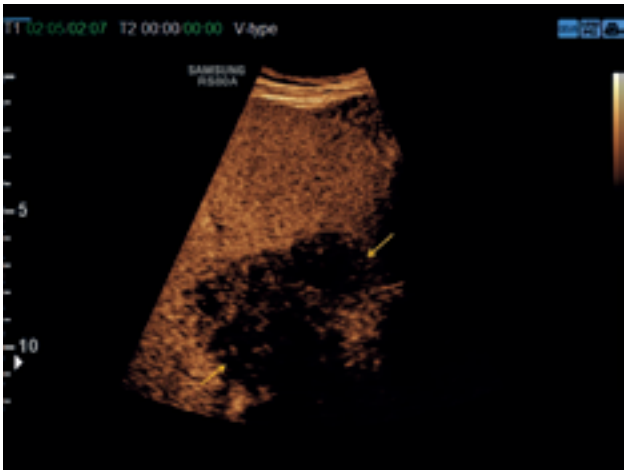

Figure 95: In the **late phase** after approx. 2 minutes, wash-out of the lesion (yellow arrows) allows it to be increasingly distinguished from the surrounding liver tissue. The lesion was confirmed by histology as a poorly-differentiated adenocarcinoma with extensive infiltration of the hepatic sinusoids. These findings were consistent with cholangiocarcinoma.

Case review 5

Figure 96: Same patient as in Figures 91–95. Intrahepatic lesion (yellow arrows) and resulting expansion of the bile ducts (red arrow).

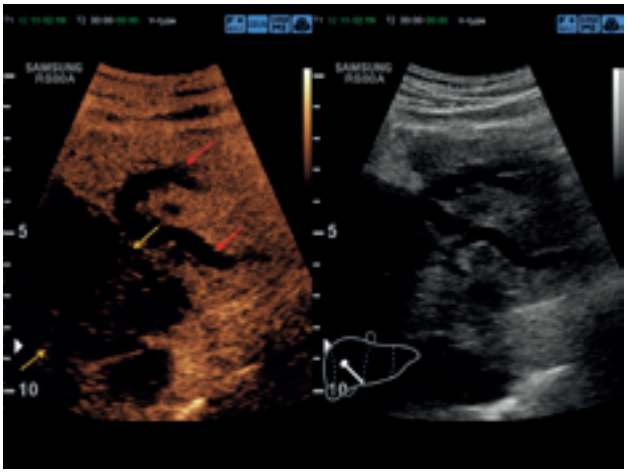

Figure 97: In the **late phase** after approx. 3 minutes, the dilated bile ducts (red arrows) and the cholangiocarcinoma (yellow arrows) are easily visible.

Case review 6

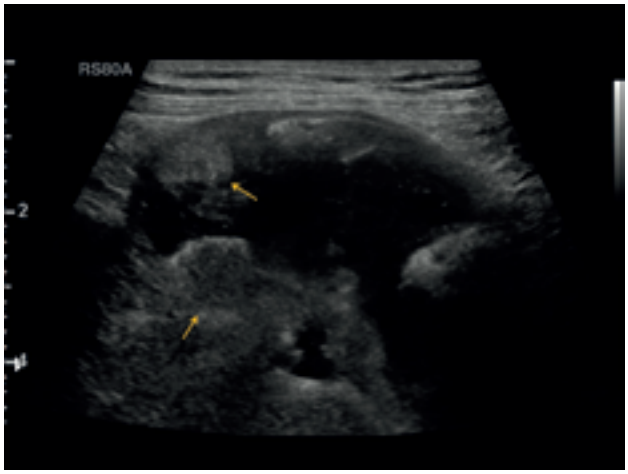

Figure 98: 91-year-old male patient with a suspicious parietal mass in the gallbladder (yellow arrows).

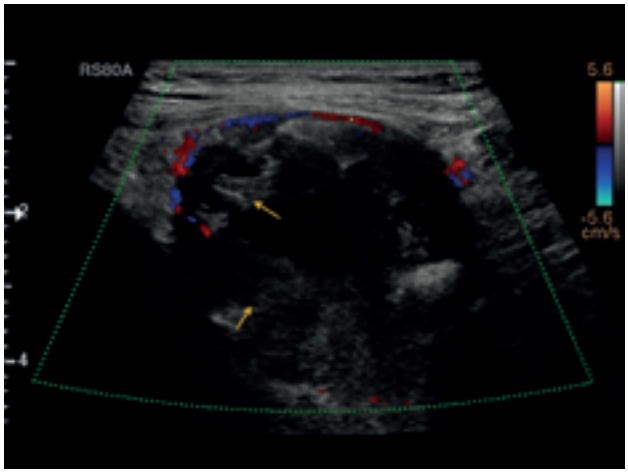

Figure 99: The lesion (yellow arrows) does not display any increase in vascularization in color duplex sonography. The gallbladder wall is delineated by a semi-circular blood vessel.

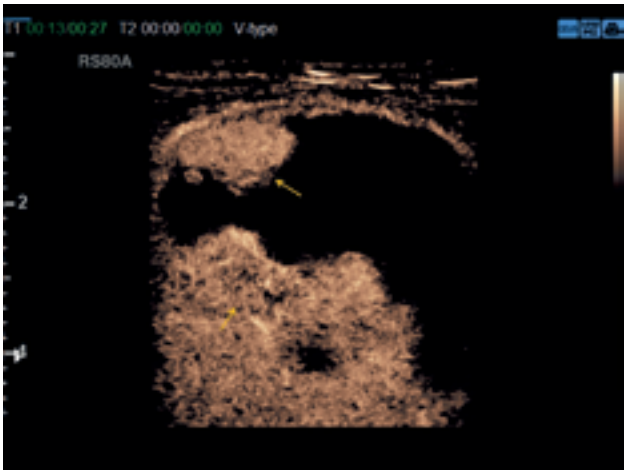

Figure 100: Contrast-enhanced ultrasound. In the **arterial phase**, this lesion (yellow arrows) is delineated by intense enhancement.

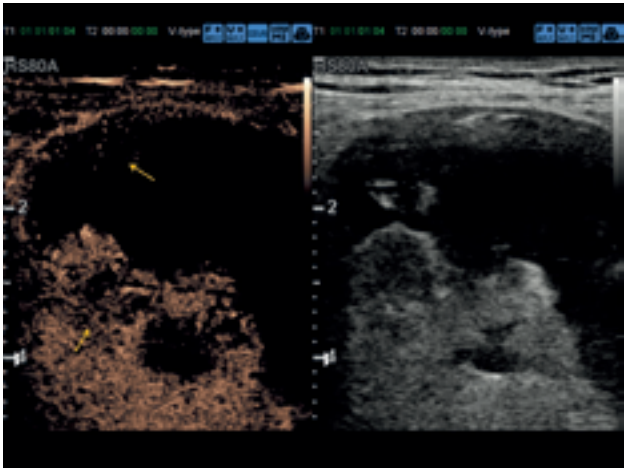

Figure 101: In the **portal venous phase** after approx. 1 minute, wash-out of the lesion (yellow arrows) already allows it to be distinguished from the surrounding liver tissue. The lesion was confirmed by histology as a tumor of the gallbladder.

3.6 Combined hepatocellular-cholangiocarcinoma

Combined hepatocellular-cholangiocarcinoma (HCC-CCC) is a rare form of liver cancer. It is a primary liver tumor that exhibits characteristics of both hepatocellular and cholangiocellular carcinomas (Figs. 102–110).

The widely-used World Health Organization (WHO) classification scheme subdivides HCC-CCC into a classical subtype and a subtype with stem cell features [Akiba et al. 2013; Sasaki et al. 2015; Wengert et al. 2015].

3.6.1 Case reviews – Combined hepatocellular-cholangiocarcinoma

Case review 1

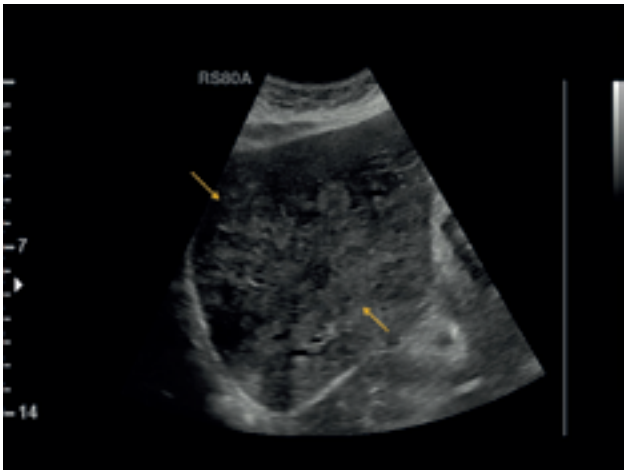

Figure 102: 69-year-old male patient with a large intrahepatic lesion (yellow arrows).

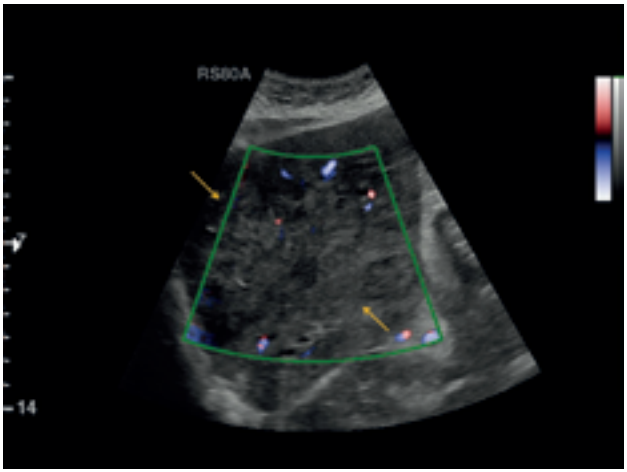

Figure 103: The lesion (yellow arrows) does not display any increase in vascularization in power Doppler ultrasound.

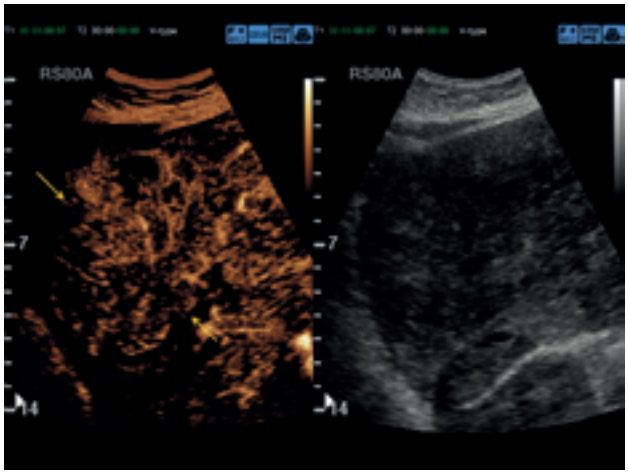

Figure 104: Contrast-enhanced ultrasound. In the **arterial phase**, the lesion is delineated by moderate enhancement.

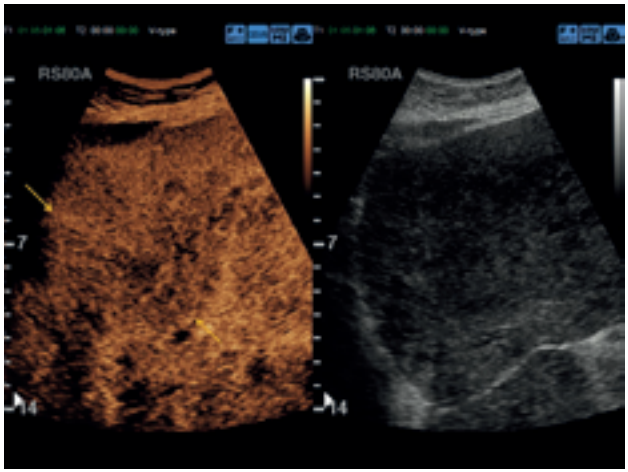

Figure 105: In the **portal venous phase** after approx. 1 minute, wash-out of the lesion (yellow arrows) already allows it to be distinguished from the surrounding liver tissue.

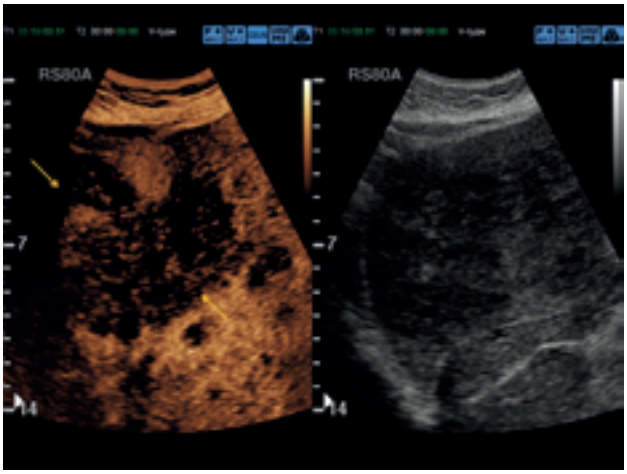

Figure 106: In the **late phase** after approx. 3:50 minutes, wash-out of the lesion (yellow arrows) allows it to be increasingly distinguished from the surrounding liver tissue. Additional satellite lesions are also enhanced. The lesion was confirmed by histology as primary combined hepatocellular-cholangiocarcinoma of the liver.

Case review 2

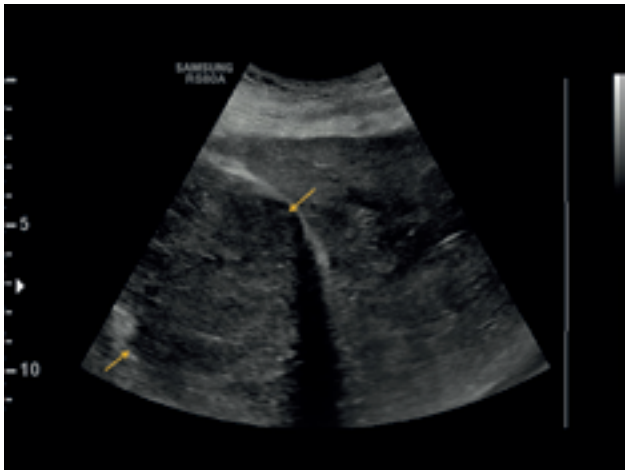

Figure 107: 69-year-old male patient with a large intrahepatic lesion (yellow arrows).

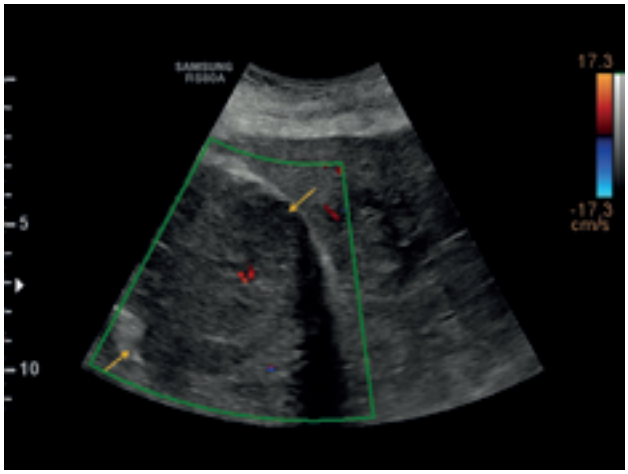

Figure 108: The lesion (yellow arrows) does not display any increase in vascularization in color duplex sonography.

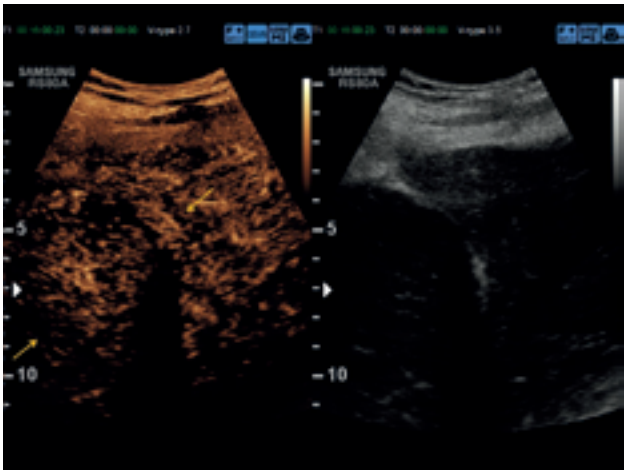

Figure 109: Contrast-enhanced ultrasound. In the **arterial phase**, the lesion is delineated by moderate enhancement.

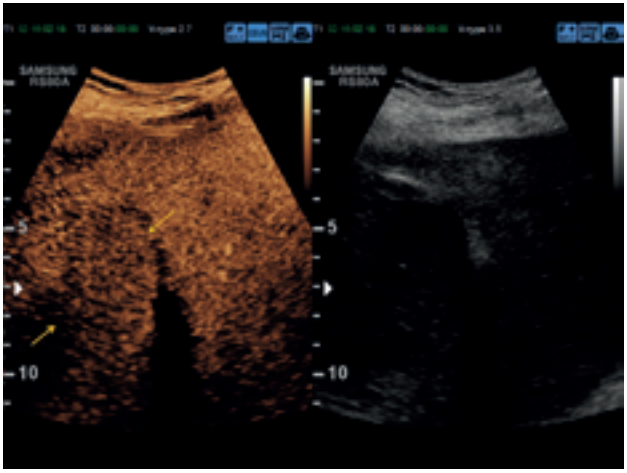

Figure 110: In the **late phase** after approx. 2:20 minutes, wash-out of the lesion (yellow arrows) allows it to be increasingly distinguished from the surrounding liver tissue. The lesion was confirmed by histology as a poorly-differentiated combined hepatocellular-cholangiocarcinoma.

4 Summary and conclusion

Contrast-enhanced ultrasound (CEUS) has a high degree of diagnostic accuracy for differentiating between benign and malignant liver lesions owing to the three vascular phases of the liver. By evaluating the vascularization of tumors in real time, this method allows liver lesions to be assessed with a high level of diagnostic reliability. During the portal venous and late phases, malignant liver lesions typically display a hypovascular appearance following wash-out of contrast agent.

As their blood supply originates from the hepatic artery, liver metastases display a typical accumulation of contrast agent during the arterial phase and an absence of enhancement during the portal venous phase.

Hepatocellular carcinoma (HCC) typically exhibits intense enhancement during the arterial phase, which then diminishes to the level of the surrounding parenchyma during the portal venous phase and is washed out during the late phase.

Cholangiocarcinoma takes up less contrast agent than HCC and at a later time point after administration, and exhibits a more rapid wash-out. CEUS thus represents a logical addition to cross-sectional imaging techniques for liver lesions which cannot be conclusively identified using these other modalities.

Owing to its lack of hepatotoxicity and nephrotoxicity and to the absence of any effects on thyroid function, CEUS is also suitable for closely monitoring response to treatment. The limiting factors of this method include patients with obesity or abdominal distension as well any lack of experience by the examining physician.

5 Literature

Akiba J, Nakashima O, Hattori S, Tanikawa K, Takenaka M, Nakayama M, et al. Clinicopathologic analysis of combined hepatocellular-cholangiocarcinoma according to the latest WHO classification. Am J Surg Pathol. 2013;37(4):496–505.

Bismuth H, Nakache R, Diamond T. Management strategies in resection for hilar cholangiocarcinoma. Ann Surg. 1992;215(1):31–8.

Blechacz B, Gores GJ. Cholangiocarcinoma: advances in pathogenesis, diagnosis, and treatment. Hepatology. 2008a;48(1):308–21.

Blechacz BR, Gores GJ. Cholangiocarcinoma. Clin Liver Dis. 2008b;12(1):131–50, ix.

Bloom CM, Langer B, Wilson SR. Role of US in the detection, characterization, and staging of cholangiocarcinoma. Radiographics. 1999;19(5):1199–218.

Boozari B, Soudah B, Rifai K, Schneidewind S, Vogel A, Hecker H, et al. Grading of hypervascular hepatocellular carcinoma using late phase of contrast enhanced sonography – a prospective study. Dig Liver Dis. 2011;43(6):484–90.

Bosch FX, Ribes J, Díaz M, Cléries R. Primary liver cancer: worldwide incidence and trends. Gastroenterology. 2004;127(5 Suppl 1):S5–16.

Chen LD, Xu HX, Xie XY, Lu MD, Xu ZF, Liu GJ, et al. Enhancement patterns of intrahepatic cholangiocarcinoma: comparison between contrast-enhanced ultrasound and contrast-enhanced CT. Br J Radiol. 2008;81(971):881–9.

Chen LD, Xu HX, Xie XY, Xie XH, Xu ZF, Liu GJ, et al. Intrahepatic cholangiocarcinoma and hepatocellular carcinoma: differential diagnosis with contrast-enhanced ultrasound. Eur Radiol. 2010;20(3):743–53.

Chiorean L, Tana C, Braden B, Caraiani C, Sparchez Z, Cui XW, et al. Advantages and Limitations of Focal Liver Lesion Assessment with Ultrasound Contrast Agents: Comments on the European Federation of Societies for Ultrasound in Medicine and Biology (EFSUMB) Guidelines. Med Princ Pract. 2016;25(5):399–407.

Choi BI, Lee JM, Kim TK, Dioguardi Burgio M, Vilgrain V. Diagnosing Borderline Hepatic Nodules in Hepatocarcinogenesis: Imaging Performance. Am J Roentgenol. 2015;205(1):10–21.

Claessen MM, Vleggaar FP, Tytgat KM, Siersema PD, van Buuren HR. High lifetime risk of cancer in primary sclerosing cholangitis. J Hepatol. 2009;50(1):158–64.

Claudon M, Tranquart F, Evans DH, Lefèvre F, Correas M. Advances in ultrasound. Eur Radiol. 2002;12(1):7–18.

Claudon M, Dietrich CF, Choi BI, Cosgrove DO, Kudo M, Nolsøe CP, et al. Guidelines and good clinical practice recommendations for Contrast Enhanced Ultrasound (CEUS) in the liver – update 2012: A WFUMB-EFSUMB initiative in cooperation with representatives of AFSUMB, AIUM, ASUM, FLAUS and ICUS. Ultrasound Med Biol. 2013;39(2):187–210.

Clevert DA, Jung EM, Stock KF, Weckbach S, Feuerbach S, Reiser M, et al. Evaluation of malignant liver tumors: biphasic MS-CT versus quantitative contrast harmonic imaging ultrasound. Z Gastroenterol. 2009;47(12):1195–202.

Clevert DA, Helck A, Paprottka PM, Schwarz F, Reiser MF. Die letzten Entwicklungen beim Ultraschall der Leber. Radiologe. 2011;51(8):661–70.

Clevert DA, D'Anastasi M, Jung EM. Contrast-enhanced ultrasound and microcirculation: efficiency through dynamics – current developments. Clin Hemorheol Microcirc. 2013;53(1–2):171–86.

Craig JR, Peters RL, Edmondson HA, Omata M. Fibrolamellar carcinoma of the liver: a tumor of adolescents and young adults with distinctive clinico-pathologic features. Cancer. 1980;46(2):372–9.

Davila JA, Morgan RO, Shaib Y, McGlynn KA, El-Serag HB. Diabetes increases the risk of hepatocellular carcinoma in the United States: a population based case control study. Gut. 2005;54(4):533–9.

D'Onofrio M, Vecchiato F, Cantisani V, Barbi E, Passamonti M, Ricci P, et al. Intrahepatic peripheral cholangiocarcinoma (IPCC): comparison between perfusion ultrasound and CT imaging. Radiol Med. 2008;113(1):76–86.

Dörffel Y, Wermke W. Neuroendocrine tumors: characterization with contrast-enhanced ultrasonography. Ultraschall Med. 2008;29(5):506–14.

El-Serag HB. Hepatocellular carcinoma. N Engl J Med. 2011;365(12):1118–27.

Epstein BE, Pajak TF, Haulk TL, Herpst JM, Order SE, Abrams RA. Metastatic nonresectable fibrolamellar hepatoma: prognostic features and natural history. Am J Clin Oncol. 1999;22(1):22–8.

Evert M, Dombrowski F. Hepatozelluläre Karzinome in der nichtzirrhotischen Leber. Pathologe. 2008;29(1):47–52.

Ferlay J, Shin HR, Bray F, Forman D, Mathers C, Parkin DM. Estimates of worldwide burden of cancer in 2008: GLOBOCAN 2008. Int J Cancer. 2010;127(12):2893–917.

Greis C. Ultrasound contrast agents as markers of vascularity and microcirculation. Clin Hemorheol Microcirc. 2009;43(1–2):1–9.

Güthle M, Dollinger MM. Epidemiologie und Risikofaktoren des hepatozellulären Karzinoms. Radiologe. 2014;54(7):654–9.

Harder J. Gallengangstumoren. In: Falk Gastro-Kolleg; Heft 4. Freiburg: Falk Foundation e.V.; 2009; S. 5–16.

Harvey CJ, Blomley MJ, Eckersley RJ, Cosgrove DO. Developments in ultrasound contrast media. Eur Radiol. 2001;11(4):675–89.

Jemal A, Bray F, Center MM, Ferlay J, Ward E, Forman D. Global cancer statistics. CA Cancer J Clin. 2011;61(2):69–90.

Jones EC, Chezmar JL, Nelson RC, Bernardino ME. The frequency and significance of small (less than or equal to 15 mm) hepatic lesions detected by CT. Am J Roentgenol. 1992;158(3):535–9.

Jung EM, Wiggermann P, Stroszczynski C, Reiser MF, Clevert DA. Sonographische Diagnostik diffuser Lebererkrankungen. Radiologe. 2012;52(8):706–16.

Jung EM, Clevert DA. Kontrastmittelsonographie (CEUS) und Bildfusion zur Durchführung von Leberinterventionen. Radiologe. 2018;58(6):538–44.

Khan SA, Thomas HC, Davidson BR, Taylor-Robinson SD. Cholangiocarcinoma. Lancet. 2005;366(9493):1303–14. Erratum in: Lancet. 2006;367(9523):1656.

Kinkel K, Lu Y, Both M, Warren RS, Thoeni RF. Detection of hepatic metastases from cancers of the gastrointestinal tract by using noninvasive imaging methods (US, CT, MR imaging, PET): a meta-analysis. Radiology. 2002;224(3):748–56.

Kobayashi M, Ikeda K, Saitoh S, Suzuki F, Tsubota A, Suzuki Y, et al. Incidence of primary cholangiocellular carcinoma of the liver in japanese patients with hepatitis C virus-related cirrhosis. Cancer. 2000;88(11):2471–7.

Ladam-Marcus V, Mac G, Job L, Piot-Veron S, Marcus C, Hoeffel C. [Contrast-enhanced ultrasound and liver imaging: review of the literature]. J Radiol. 2009;90(1 Pt 2):93–106; quiz 107–8.

Leitlinienprogramm Onkologie. S3-Leitlinie hepatozelluläres Karzinom / Mai 2013 (Deutsche Krebsgesellschaft, Deutsche Krebshilfe, AWMF): Diagnostik und Therapie des hepatozellulären Karzinoms, Langversion 1.0, AWMF Registrierungsnummer: 032-053OL, http://leitlinienprogramm-onkologie.de/Leitlinien.7.0.html

Lindner JR, Song J, Jayaweera AR, Sklenar J, Kaul S. Microvascular rheology of Definity microbubbles after intra-arterial and intravenous administration. J Am Soc Echocardiogr. 2002;15(5):396–403.

Marrero JA, Fontana RJ, Su GL, Conjeevaram HS, Emick DM, Lok AS. NAFLD may be a common underlying liver disease in patients with hepatocellular carcinoma in the United States. Hepatology. 2002;36(6):1349–54.

McLarney JK, Rucker PT, Bender GN, Goodman ZD, Kashitani N, Ros PR. Fibrolamellar carcinoma of the liver: radiologic-pathologic correlation. Radiographics. 1999;19(2):453–71.

Meacock LM, Sellars ME, Sidhu PS. Evaluation of gallbladder and biliary duct disease using microbubble contrast-enhanced ultrasound. Br J Radiol. 2010;83(991):615–27.

Müller-Peltzer K, Rübenthaler J, Reiser M, Clevert DA. Kontrastverstärkter Ultraschall (CEUS) der Leber: kritische Bewertung des Einsatzes in der Routinediagnostik. Radiologe. 2017;57(5):348–55.

Müller-Peltzer K, Rübenthaler J, Negrão de Figueiredo G, Clevert DA. CEUS –Diagnostik benigner Leberläsionen. Radiologe. 2018;58(6):521–7.

Nagorney DM, Donohue JH, Farnell MB, Schleck CD, Ilstrup DM. Outcomes after curative resections of cholangiocarcinoma. Arch Surg. 1993;128(8):871–7; discussion 877–9.

Nakeeb A, Pitt HA, Sohn TA, Coleman J, Abrams RA, Piantadosi S, et al. Cholangiocarcinoma. A spectrum of intrahepatic, perihilar, and distal tumors. Ann Surg. 1996;224(4):463–73; discussion 473–5.

Negrão de Figueiredo G, Müller-Peltzer K, Rübenthaler J, Clevert DA. CEUS – Diagnostik maligner Leberläsionen. Radiologe. 2018;58(6):528–37.

Nicolau C, Vilana R, Catalá V, Bianchi L, Gilabert R, García A, et al. Importance of evaluating all vascular phases on contrast-enhanced sonography in the differentiation of benign from malignant focal liver lesions. Am J Roentgenol. 2006;186(1):158–67.

Ochs A. Sonografie der Leber. 27. Auflage. Freiburg: Falk Foundation e.V.; 2014.

Oldenburg A, Hohmann J, Foert E, Skrok J, Hoffmann CW, Frericks B, et al. Detection of hepatic metastases with low MI real time contrast enhanced sonography and SonoVue. Ultraschall Med. 2005;26(4):277–84.

Piscaglia F, Bolondi L; Italian Society for Ultrasound in Medicine and Biology (SIUMB) Study Group on Ultrasound Contrast Agents. The safety of Sonovue in abdominal applications: retrospective analysis of 23188 investigations. Ultrasound Med Biol. 2006;32(9):1369–75.

Poultsides GA, Zhu AX, Choti MA, Pawlik TM. Intrahepatic cholangiocarcinoma. Surg Clin North Am. 2010;90(4):817–37.

Prokop M, Galanski M, van der Molen AJ, Schaefer-Prokop C, editors. Spiral and Multislice Computed Tomography of the Body. Stuttgart, New York: Thieme Verlag; 2003.

Regge D, Campanella D, Anselmetti GC, Cirillo S, Gallo TM, Muratore A, et al. Diagnostic accuracy of portal-phase CT and MRI with mangafodipir trisodium in detecting liver metastases from colorectal carcinoma. Clin Radiol. 2006;61(4):338–47.

Rizvi S, Gores GJ. Pathogenesis, diagnosis, and management of cholangiocarcinoma. Gastroenterology. 2013;145(6):1215–29.

Rubens DJ. Ultrasound Imaging of the Biliary Tract. Ultrasound Clin. 2007;2:391–413.

Samaras P, Geier A, Riesterer O, Dutkowksi P. Tumore des biliären Trakts: Häufigkeit, Diagnostik und Therapie. Schweizer Zeitschrift für Onkologie. 2011;2:26–31.

Sasaki M, Sato H, Kakuda Y, Sato Y, Choi JH, Nakanuma Y. Clinicopathological significance of ‚subtypes with stem-cell feature' in combined hepatocellular-cholangiocarcinoma. Liver Int. 2015;35(3):1024–35.

Schellhaas B, Wildner D, Pfeifer L, Goertz RS, Hagel A, Neurath MF, et al. LI-RADS-CEUS – Proposal for a Contrast-Enhanced Ultrasound Algorithm for the Diagnosis of Hepatocellular Carcinoma in High-Risk Populations. Ultraschall Med. 2016;37(6):627–34.

Shah S, Shukla A, Paunipagar B. Radiological features of hepatocellular carcinoma. J Clin Exp Hepatol. 2014;4(Suppl 3):S63–6.

Shaib Y, El-Serag HB. The epidemiology of cholangiocarcinoma. Semin Liver Dis. 2004;24(2):115–25.

Spangenberg HC, Thimme Robert, Blum HE. Der Leberrundherd. Dtsch Arztebl 2007;104(33): A 2279–88.

Starley BQ, Calcagno CJ, Harrison SA. Nonalcoholic fatty liver disease and hepatocellular carcinoma: a weighty connection. Hepatology. 2010;51(5):1820–32.

Strobel DB. Diagnostik bei fokalen Leberläsionen. Dtsch Arztebl. 2006;103(12):789–93.

Strobel D, Seitz K, Blank W, Schuler A, Dietrich C, von Herbay A, et al. Contrast-enhanced ultrasound for the characterization of focal liver lesions – diagnostic accuracy in clinical practice (DEGUM multicenter trial). Ultraschall Med. 2008;29(5):499–505.

Strobel D, Bernatik T, Blank W, Schuler A, Greis C, Dietrich CF, et al. Diagnostic accuracy of CEUS in the differential diagnosis of small (≤20 mm) and subcentimetric (≤10 mm) focal liver lesions in comparison with histology. Results of the DEGUM multicenter trial. Ultraschall Med. 2011;32(6):593–7.

Trenker C, Kunsch S, Michl P, Wissniowski TT, Goerg K, Goerg C. Contrast-enhanced ultrasound (CEUS) in hepatic lymphoma: retrospective evaluation in 38 cases. Ultraschall Med. 2014;35(2):142–8.

Vogel A, Wege H, Caca K, Nashan B, Neumann U. The Diagnosis and Treatment of Cholangiocarcinoma. Dtsch Arztebl Int 2014;111(44):748–54.

Wang W, Fei Y, Wang F. Meta-analysis of contrast-enhanced ultrasonography for the detection of gallbladder carcinoma. Med Ultrason. 2016,18(3):281–7.

Welzel TM, Graubard BI, Zeuzem S, El-Serag HB, Davila JA, McGlynn KA. Metabolic syndrome increases the risk of primary liver cancer in the United States: a study in the SEER-Medicare database. Hepatology. 2011;54(2):463–71.

Wengert GJ, Bickel H, Breitenseher J, Ba-Ssalamah A. Primäre Lebertumoren: Hepatozelluläres vs. intrahepatisches cholangiozelluläres Karzinom. Radiologe. 2015;55(1):27–35.

Wermke W. Sonographische Differenzialdiagnose – Leberkrankheiten. Köln: Deutscher Ärzte-Verlag; 2006. S. 233, 358–61.

Weskott HP. Kontrastverstärkter Ultraschall [German version of: Contrast-enhanced ultrasound, CEUS]. Bremen: Uni-Med Verlag; 2010. S. 94.

Weskott HP. Nachweis und Charakterisierung von Lebermetastasen. Radiologe. 2011;51(6):469–74.

Wildner D, Bernatik T, Greis C, Seitz K, Neurath MF, Strobel D. CEUS in hepatocellular carcinoma and intrahepatic cholangiocellular carcinoma in 320 patients – early or late washout matters: a subanalysis of the DEGUM multicenter trial. Ultraschall Med. 2015;36(2):132–9.

Xu HX, Lu MD, Liu GJ, Xie XY, Xu ZF, Zheng YL, et al. Imaging of peripheral cholangiocarcinoma with low-mechanical index contrast-enhanced sonography and SonoVue: initial experience. J Ultrasound Med. 2006;25(1):23–33.

Yen CL, Jeng CM, Yang SS. The benefits of comparing conventional sonography, real-time spatial compound sonography, tissue harmonic sonography, and tissue harmonic compound sonography of hepatic lesions. Clin Imaging. 2008;32(1):11–5.

Zajaczek JE, Keberle M. Stellenwert der radiologischen Verfahren bei Erkrankungen von Gallenblase und -wegen. Radiologe. 2005;45(11):976–8, 980–6.

Zhou XD, Tang ZY, Fan J, Zhou J, Wu ZQ, Qin LX, et al. Intrahepatic cholangiocarcinoma: report of 272 patients compared with 5,829 patients with hepatocellular carcinoma. J Cancer Res Clin Oncol. 2009;135(8):1073–80.

FALK FOUNDATION e.V.

Leinenweberstr. 5
79108 Freiburg
Germany

U42-2e 1-1/2020 POP